

(Gibco, Grand Island, NY, USA) supplemented with 10% fetal bovine serum (FBS) (Sigma, St. Louis, MO, USA) and an antibiotic/antimycotic mixture (100 U/ml each) (Gibco) and were cultured in a humidified incubator (5% CO₂) at 37°C. The medium was replaced with fresh medium every 3–4 days. Prior to each experiment, the cells were seeded into 6- or 12-well plates and allowed to attach for at least 24 hr (6-well for triglyceride [TG] assay and 12-well for RNA extraction).

Transfection. Using SuperFect Transfection Reagent (Qiagen, Tokyo), cells were transfected with 4 or 3 µg of pCAG-HCVcore or pCAG-MOK (4 µg for 6-well plates and 3 µg for 12-well plates) and were cultured in DMEM with 10% FBS. After 24 or 48 hr, the cells were harvested for analysis. The efficiency of transfection was investigated using pCAG-LacZ. Cells were washed with phosphate-buffered saline (PBS) and fixed with 2% formaldehyde and 0.2% glutaraldehyde in PBS. Then the cells were stained with X-gal using a β-Gal Staining Set (Roche, Tokyo).

Animals. Adult male C57BL/6 mice (Charles River Laboratories, Yokohama, Japan), which were over 8 weeks old and weighed 21–24 g, were used in this study. All animals were housed in an environmentally controlled facility with a 12-hr lighting time (lights on from 0700 until 1900 hr). They were given free access to standard chow and water. Experiments (intravenous injection and sacrifice) were performed from 0900 to 21 hr. The animals received humane care according to the institutional guidelines for handling experimental animals.

HCV Core Protein Expression in Mice. The animals received an intravenous injection of 1×10^9 pfu (plaque-forming units) of AdexCAHCVcore or AdexCALacZ and were sacrificed 3 days later. Mice were anesthetized with pentobarbital (100 mg/kg intraperitoneally). Blood was collected by cardiac puncture with a heparinized syringe, after which the liver was rapidly removed, weighed, and perfused with ice-cold PBS (pH 7.4). Part of the liver was fixed in 10% neutral buffered formalin and embedded in paraffin for histologic analysis. Another part was stored in RNA later reagent (Qiagen, Tokyo) at 4°C for extraction of RNA, and the remaining liver tissue was snap-frozen in liquid nitrogen and stored at –80°C until required. Plasma was immediately separated by centrifugation (10,000 rpm at 4°C) and stored at –20°C.

Liver Histology and Serum ALT Level. Sections of liver tissue (4 µm thick) were stained with hematoxylin and eosin for analysis. The serum alanine aminotransferase (ALT) level was measured using an automated technique by SRL Co. (Hiroshima, Japan).

HCV Core Protein Expression in Cells. Proteins were extracted from cells using PRO-PREP protein extraction solution (containing 1.0 mM PMSF, 1.0 mM EDTA, 1 µM pepstatin, 1 µM leupeptin, and 1 µM aprotinin) (Intron Biotechnology, Kyungki-Do, Korea). HCV core antigen levels were measured in cells using an HCV core antigen enzyme-linked immunosorbent assay (ELISA) (Ortho-Clinical Diagnostics K.K., Tokyo).

HCV Core Protein Expression in Mice. We confirmed HCV core protein expression in liver tissue by Western blot analysis. Proteins were extracted using PRO-PREP protein extraction solution. Then 50 µg of protein was separated by sodium dodecyl sulfate–polyacrylamide gel electrophoresis and transferred to a nitrocellulose membrane (Millipore, Bedford, MA, USA) using a tank blotting system according to the manufacturer's instructions (Bio-Rad Laboratories). After transfer, the membrane was blocked for 2 hr at room temperature with 5%

powdered skim milk dissolved in Tris-buffered saline containing 0.05% between 20 and then incubated overnight at 4°C with a monoclonal mouse antibody to HCV core protein (kindly provided by Ortho-Clinical Diagnostics K.K.). Immune complexes were detected using alkaline phosphatase-conjugated anti-mouse IgG (Cosmo Bio, Tokyo) according to the manufacturer's instructions (Bio-Rad Laboratories). Detection of HCV core protein was performed by comparison with the following standards: myosin (200 kDa), β-galactosidase (116 kDa), bovine serum albumin (66 kDa), carbonic anhydrase (31 kDa), soybean trypsin inhibitor (21.5 kDa), lysozyme (14.4 kDa), and aprotinin (6.5 kDa).

Measurement of Triglyceride Content. After the medium was removed, the cells were washed three times with PBS and resuspended in 200 µl of PBS. Then lipids were extracted from 100 µl of PBS by the method of Bligh and Dyer (27) and resuspended in 100 µL of 10% Triton X. The cellular content of TG was measured using enzyme reagents and standards from Wako (Osaka, Japan). The remainder of the PBS suspension was used for the protein assay. In mice experiments, livers were homogenized in PBS and 100 µl of the homogenate was used for extraction of lipids. Total protein was measured with protein assay reagents from Bio-Rad (Richmond, CA, USA).

Hepatic Level of Thiobarbituric Acid-Reactive Substances (TBARS). The hepatic level of TBARS was measured using an OXI-TEK TBARS Assay Kit (Zeptomatrix Corporation, New York, USA). Briefly, 100 mg of liver tissue was homogenized in 10 vol of normal saline. Then 100 µl of SDS and 2.5 ml of TBA/buffer reagent were added to 100 µl of this homogenate or the malondialdehyde standard. Samples were incubated at 95°C for 60 min, cooled in an ice bath for 10 min, and centrifuged at 3000 rpm for 15 min, after which the supernatant was analyzed by spectrophotometry (532 nm).

Extraction of RNA and RT-PCR. The medium was removed and the cells were washed twice with PBS. After centrifugation, total RNA was isolated using an RNeasy Mini Kit (Qiagen, Tokyo). From mouse, 20 mg of liver tissue was used for RNA extraction. Then 2 µg of total RNA was employed for reverse transcription using random hexamers (final concentration: 2.5 µM) and murine leukemia virus reverse transcriptase (final concentration: 2.5 U/µl) (Roche, Tokyo). Specific primer sets were synthesized for performance of the PCR (Table 1) and were used for assessment of liver-predominant mitochondrial carnitine palmitoyl transferase-1 (CPT1A in humans and CPT1 in mice; the rate-limiting enzyme of mitochondrial β-oxidation), acyl-CoA oxidase (ACO1 in humans and AOX in mice; the rate-limiting enzyme of peroxisomal β-oxidation), cytochrome P-450 4A11 (CYP4A11; involved in microsomal ω-oxidation), multidrug resistance protein 3 (MDR3 in humans and Mdr2 in mice; an ABC transporter and phospholipid flip-flop), microsomal TG transfer protein (MTP; a vital protein for TG incorporation into VLDL), and two nuclear receptors (peroxisome proliferator-activated receptor α [PPARα]) and peroxisome proliferator-activated receptor γ (PPARγ). Roles of these genes are summarized in Table 2. Amplification involved 30 cycles of denaturation at 95°C for 60 sec, annealing at each specified temperature (Table 1) for 30 sec, and extension at 72°C for 60 sec. The reaction products were analyzed on a 2% agarose gel and were visualized by ethidium bromide staining. The PCR products were excised from the gel, purified using a gel purification kit (Qiagen), and quantified by spectrophotometry. Dilutions

TABLE 1. PRIMER SETS IN THE EXPERIMENTS

	Forward	Reverse	Annealing temp. (°C)
Human			
GAPDH	GAACGGGAAGCTCACTGGCATGGC	TGAGGTCCACCCTGTTGCTG	65
PPAR α	GGAAAGCCCCTCTGCCCT	AGTCACCGAGGAGGGGCTCGA	63
PPAR γ	CATTCTGGCCACCAACTTTGG	TGGAGATGCAGGCTCCACTTTG	63
MDR3 (ABCB4)	GATGAAAAGGCTGCCACTAG	TTGCACTTCTGCTGCTTAC	62
MTP	GGCTAGCCTATTTTCAGACACA	GATGAGCCTGGTAGGTCCT	60
CPT1A	AGACGGTGGAAACAGAGGCTGAAG	TGAGACCAAACAAAGTGATGATGTCAG	67
ACO1	GGGCATGGCTATTCTCATTGC	CGAACAAAGGTCAACAGAAGTTAGGTTT	60
CYP4A11	GTGGCCCAACCCAGAGGT	TCCCAATGCAGTTCCTTGATC	55
Mouse			
GAPDH	AGAACATCCCTGCATCC	TTGTCATGAGAGCAATGCC	56
PPAR α	TGCAGAGCAACCATCCAG	TAATGGCGAATTATAAAC	50
PPAR γ	GGTGAAACTCTGGGAGATT	CAACCAITGGGTCACTCTT	59
Mdr2 (Abcb4)	TATCCGCTATGGCCGTGGGAA	ATCGGTGAGCTATCACAATGG	56
MTP	TGAGCGGTATACAAGCTCAC	CTGGAAGATGCTTCTCTCGC	60
LCPT	CGCACGGAAGGAAAATGG	TGTGCCCAATATTCCTGG	52
AOX	CTTGTTCCGCAAGTGAGG	CAGGATCCGACTGTTTACC	56

ranging from 3×10^{-5} to 3×10^2 pg were prepared in water and used as the standards.

Quantitative PCR. Quantitative PCR was performed using the Light-Cycler Fast-Start DNA Master SYBR Green system (Roche Molecular Biochemicals, Tokyo). PCR was carried out in a final reaction volume of 20 μ l using 1 μ l of each primer at 10 μ M (final concentration: 0.5 μ M), 1.6 μ l of 25 mM MgCl₂ (final concentration: 3 mM), 2 μ l of the enzyme mix supplied, 12.4 μ l of H₂O, and 2 μ l of the template. The enzyme mix contained the reaction buffer, Fast-Start Taq DNA polymerase, and DNA double strand-specific SYBR Green I dye for detection of PCR products. PCR was performed in a Light-Cycler (Roche) with preincubation for 10 min at 95°C followed by 40 cycles of denaturation for 15 sec at 95°C, annealing for 5 sec at each specified temperature (see Table 1), and extension for 25 sec at 72°C, with fluorescent detection at the end of extension. Next, the PCR products were subjected to melting curve analysis to exclude the amplification of primer dimmers or other nonspecific products. If primer dimmers and nonspecific bands were detected, fluorescence detection was repeated after extension at each specified temperature for 1 sec. Analysis was carried

out with Light-Cycler 3.5 software (Roche). Quantification was done using the "point fitting" mode and baseline adjustment. The standard curve for each gene was created using five different dilutions. The plot of the number of PCR cycles versus log concentration was considered reliable when the error was <0.2.

Statistical Analysis. Results are expressed as the mean \pm SE. Statistical analysis was performed using Student's *t*-test, and *P* < 0.05 was defined as indicating significance.

RESULTS

HCV Core Protein Expression in HepG2 Cells. The transfection efficiency of pCAG-LacZ was about 20%. HCV core protein expression by the cells was confirmed using the HCV core antigen ELISA. No HCV core antigen was detected in mock-transfected and nontransfected cells. The level of HCV core protein expression showed no difference between 24 and 48 hr after transfection (24 hr,

TABLE 2. ROLES OF ANALYZED GENES IN FATTY ACID METABOLISM

MDR3	Multidrug resistance protein 3 An ABC transporter and phospholipid flippase <i>Role: Phospholipid secretion into bile</i>
MTP	Microsomal triglyceride transfer protein A vital protein for TG incorporation into VLDL <i>Role: triglyceride secretion into blood</i>
CPT1A	Liver-predominant mitochondrial carnitine palmitoyl transferase-1 The rate-limiting enzyme of mitochondrial β -oxidation <i>Role: Fatty acid β-oxidation in the liver</i>
ACO1	Acyl-CoA oxidase The rate-limiting enzyme of peroxisomal β -oxidation <i>Role: Fatty acid β-oxidation in the liver</i>
PPAR α	Peroxisome proliferator-activated receptor α A nuclear receptor <i>Role: A nuclear receptor controlling lipid metabolism-associated genes</i>
PPAR γ	Peroxisome proliferator-activated receptor γ A nuclear receptor <i>Role: A nuclear receptor controlling lipid metabolism-associated genes</i>

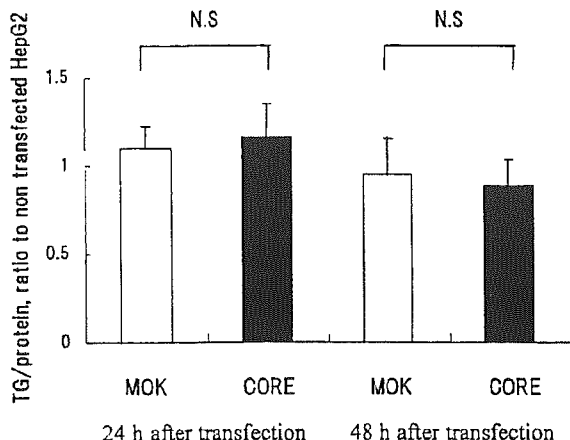


Fig 2. Effect of HCV core protein expression on cellular triglyceride (TG) content. Four micrograms of pCAG-MOK (control) or pCAG-HCVcore was transfected into HepG2 cells cultured in six-well plates by the lipofection method. At 24 or 48 hr after transfection, cells were collected for protein assay and lipid extraction. TG content was measured and expressed as the ratio to the protein content. Data are shown as values relative to those for nontransfected HepG2 cells. Each data point represents the mean \pm SD of six individual experiments. $P = NS$ compared with pCAG-MOK (Student's *t*-test).

1.31 \pm 0.20 nmol/mg protein; 48 hr, 1.25 \pm 0.16 nmol/mg protein).

TG Content of HepG2 Cells. The cellular TG content at 24 hr after transfection showed no difference between HCV core transfectants (CORE) and mock transfectants (MOK) as control (CORE, 1.16 \pm 0.19; MOK, 1.10 \pm 0.13; $P = 0.57$). At 48 hr after transfection, the TG content also showed no difference between the groups (CORE, 0.88 \pm 0.16; MOK, 0.95 \pm 0.18; $P = 0.55$). Data are expressed as the ratio to nontransfected cells (Figure 2).

Expression of Target Genes by HepG2 Cells. At 24 hr after transfection, HCV CORE showed increased expression of mRNA for PPAR γ (CORE, 2.39 \pm 0.26; MOK, 1.98 \pm 0.28; $P = 0.025$), MDR3 (CORE, 1.30 \pm 0.21; MOK, 1.02 \pm 0.20; $P < 0.01$), and ACO1 (CORE, 1.11 \pm 0.14; MOK, 0.76 \pm 0.08; $P < 0.01$) compared to MOK, while CPT (CORE, 1.18 \pm 0.16; MOK, 0.94 \pm 0.28; $P = 0.102$) and PPAR α (CORE, 0.84 \pm 0.14; MOK, 0.69 \pm 0.10; $P = 0.055$) expression was normal (Figure 3). At 48 hr after transfection, HCV CORE showed lower expression of mRNA for PPAR α (CORE, 0.89 \pm 0.02; MOK, 0.96 \pm 0.08;

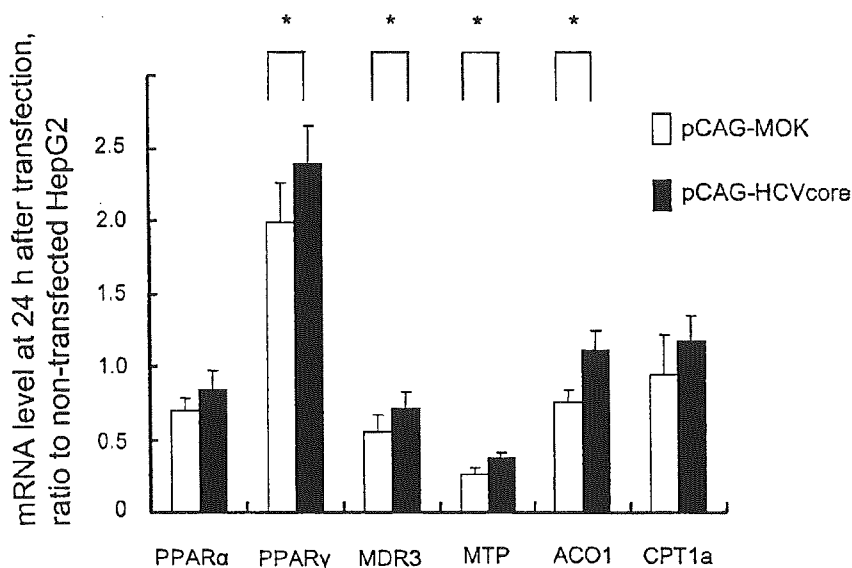


Fig 3. Effect of HCV core protein expression on mRNA levels at 24 hr after transfection. Three micrograms of pCAG-MOK (control) or pCAG-HCVcore was transfected into HepG2 cells cultured in 12-well plates by the lipofection method. At 24 hr after transfection, cells were collected for extraction of RNA. Complementary DNA was synthesized from 2 μ g of RNA and used for quantified PCR with the Light-Cycler Fast-Start DNA Master SYBR Green system. GAPDH level was measured as the internal control, and the ratio to GAPDH was calculated for each sample. Data are shown as values relative to those for nontransfected HepG2 cells. Each data point represents the mean \pm SD of 6 individual experiments. * $P < 0.05$ compared with pCAG-MOK (Student's *t*-test).

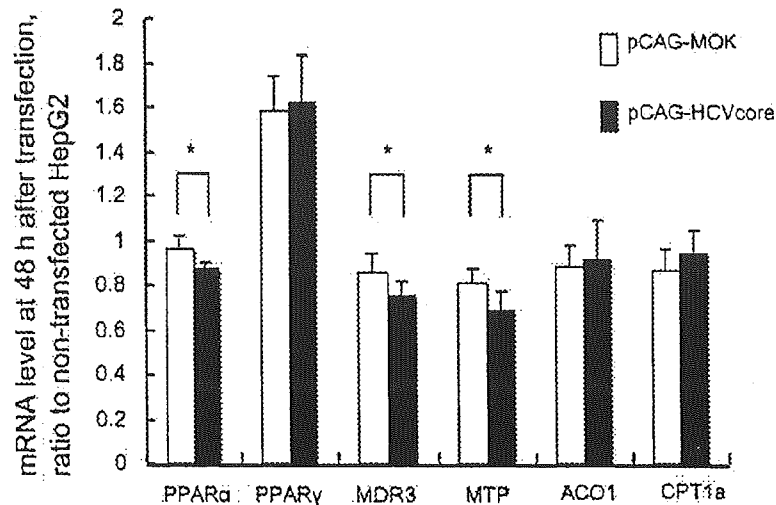


Fig 4. Effect of HCV core protein on mRNA expression at 48 hr after transfection. Three micrograms of pCAG-MOK (control) or pCAG-HCVcore was transfected into HepG2 cells cultured in 12-well plates by the lipofection method. At 48 hr after transfection, cells were collected and used for RNA extraction. Complementary DNA was synthesized from 2 μ g of RNA and used for quantified PCR with the Light-Cycler Fast-Start DNA Master SYBR Green system. GAPDH was measured as an internal control, and the ratio to GAPDH was calculated for each sample. Data are shown as values relative to those for nontransfected HepG2 cells. Each data point represents the mean \pm SD of 6 individual experiments. * $P < 0.05$ compared with pCAG-MOK (Student's *t*-test).

$P = 0.048$), MDR3 (CORE, 0.75 ± 0.06 ; MOK, 0.86 ± 0.08 ; $P = 0.031$), and MTP (CORE, 0.69 ± 0.08 ; MOK, 0.81 ± 0.07 ; $P = 0.016$) compared with MOK, while ACO1 returned to the control level (CORE, 0.91 ± 0.18 ; MOK, 0.88 ± 0.09 ; $P = 0.70$) and the CPT level was normal (CORE, 0.94 ± 0.13 ; MOK, 0.86 ± 0.10 ; $P = 0.27$). Data are expressed as the ratio to nontransfected cells (Figure 4). Experiments were repeated three times and similar results were obtained, with statistical significance. CYP4A11 was not detected by RT-PCR, so we could not make a standard for the Light-Cycler.

HCV Core Protein Expression in Mice. HCV core protein-expressing mice looked healthy and their body weight (BW) and liver weight remained within the normal range (BW [g]: PBS, 22.5 ± 0.816 ; AdexCAHCVcore (CORE), 21.7 ± 0.84 ; AdexCALacZ (LacZ), as control, 21.5 ± 0.71). Similar mild elevation of ALT and mild hepatic lymphocyte infiltration were observed in both groups of adenovirus-infected mice, showing no differences between Core and LacZ (GPT [IU/ml]: PBS, 65 ± 17.8 ; CORE, 170 ± 59.4 ; LacZ, 142.5 ± 82.2). Lipid drops were not observed in either group (data not shown). Western blot analysis revealed the HCV core protein of about 19–20 kDa (Figure 5). In preliminary experiments, animals receiving an intravenous injection of 1×10^9 pfu developed severe hepatitis after 7 days, while animals re-

ceiving 1×10^8 pfu showed a mild elevation of ALT, but their HCV core protein expression (based on quantification of mRNA and HCV core antigen) was significantly lower at 7 days after injection. Thus, we selected injection of 1×10^9 pfu and sacrifice at 3 days for the study protocol.

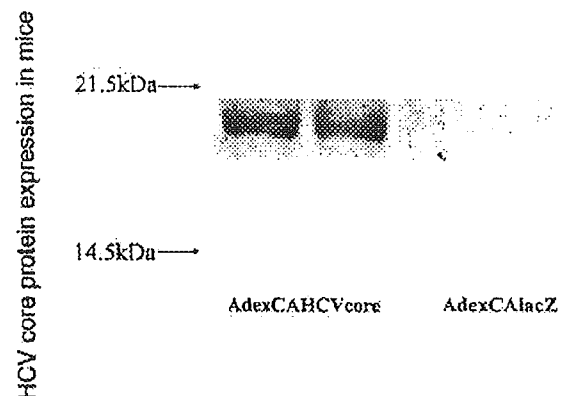


Fig 5. HCV core protein expression in mice. AdexCALacZ (control recombinant adenovirus) or AdexCAHCVcore was used to infect male C57BL/6 mice (8–10 weeks old) by intravenous administration (1×10^9 pfu). Three days after infection, livers were collected for protein assay. Using 50 μ g of protein, HCV core protein expression was confirmed by Western blotting with a mouse monoclonal antibody for HCV core protein (19–20 kDa).

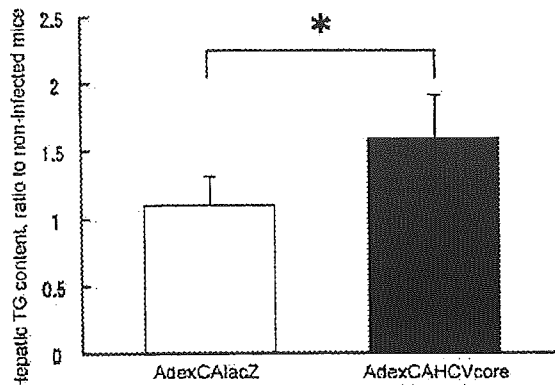


Fig 6. Effect of HCV core protein expression on the hepatic triglyceride content in mice. AdexCALacZ (control adenovirus) or AdexCAHCVcore was used to infect male C57BL/6 mice (8–10 weeks old) by intravenous administration (1×10^9 pfu). At 3 days after infection, the livers were collected and 100 μ l of liver homogenate was used for lipid extraction and for the protein assay. The TG content was measured and expressed as the ratio to the protein content. Data are shown as values relative to those for noninfected mice. Each data point represents the mean \pm SD of four individual mice. * $P < 0.05$ compared with AdexCALacZ (control adenovirus) by Student's *t*-test.

Hepatic TG Level in Mice. Animals injected with AdexCAHCVcore showed a 1.45-fold increase in hepatic TG content compared to animals injected with AdexCALacZ (CORE, 1.60 ± 0.33 ; LacZ, 1.10 ± 0.21 ; $P = 0.044$; $N = 4$). Data are expressed as the ratio to noninfected mice (Figure 6).

Expression of Target Genes in Mice. In the livers of HCV core protein-expressing mice, PPAR α (CORE, 0.59 ± 0.11 ; LacZ, 1.33 ± 0.21 ; $P < 0.01$), PPAR γ (CORE, 1.05 ± 0.10 ; LacZ, 2.43 ± 0.69 ; $P < 0.01$), Mdr2 (CORE, 0.85 ± 0.08 ; LacZ, 1.12 ± 0.12 ; $P = 0.011$), AOX (CORE, 0.235 ± 0.08 ; LacZ, 0.401 ± 0.07 ; $P = 0.02$), and CPT (CORE, 1.14 ± 0.14 ; LacZ 2.34 ± 0.51 ; $P < 0.01$) were all down-regulated, while the level of MTP mRNA was unchanged (CORE, 1.37 ± 0.08 ; LacZ, 1.24 ± 0.17 ; $P = 0.22$; $N = 4$). Data are expressed as the ratio to noninfected mice (Figure 7).

Hepatic TBARS Level. In the livers of HCV core protein-expressing mice, the TBARS level was increased compared with that in the control group (CORE, 0.84 ± 0.08 ; LacZ, 0.41 ± 0.01 ; $P < 0.01$; $N = 4$) (Figure 8).

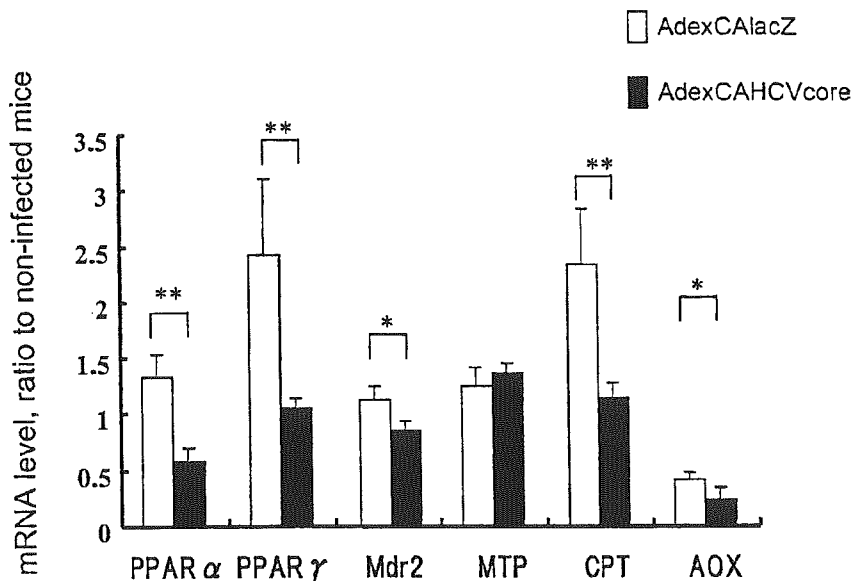


Fig 7. Effect of HCV core protein expression on mRNA levels in mice. AdexCALacZ (control adenovirus) or AdexCAHCVcore was used to infect male C57BL/6 mice (8–10 weeks old) by intravenous administration (1×10^9 pfu). At 3 days after infection, livers were collected for RNA extraction. Complementary DNA was synthesized from 2 μ g of RNA and used for quantified PCR with the Light-Cycler Fast-Start DNA Master SYBR Green system. GAPDH was measured as an internal control, and the ratio to GAPDH was calculated for each sample. Data are shown as relative values to those for noninfected mice. Each data point represents the mean \pm SD of four individual mice. * $P < 0.05$ and ** $P < 0.01$ compared with AdexCALacZ (control adenovirus) by Student's *t*-test.

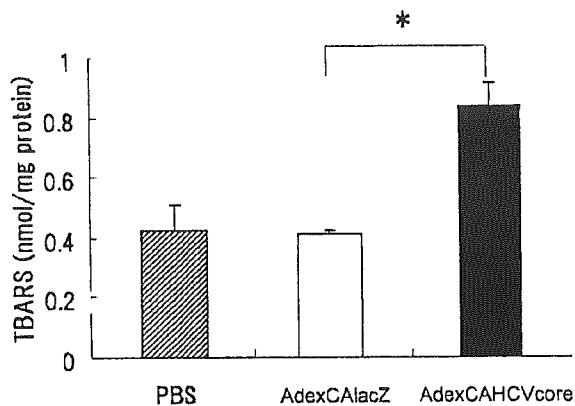


Fig 8. Effect of HCV core protein expression on TBARS in the mouse liver. AdexCALacZ (control adenovirus) or AdexCAHCVcore was used to infect male C57BL/6 mice (8–10 weeks old) by intravenous administration (1×10^9 pfu). At 3 days after infection, livers were homogenized in 10 vol of normal saline. TBARS and total protein (TP) levels were measured as described under Materials and Methods. Data are expressed as the ratio to the TP level. Each data point represents the mean \pm SD of four individual mice. * $P < 0.01$ compared with AdexCALacZ (control adenovirus) by Student's *t*-test.

DISCUSSION

HCV core protein was recently reported to cause hepatic steatosis and induction of reactive oxygen species (ROS) in an HCV core protein transgenic mouse model (18–20). In the transgenic mouse model, it was also shown that a decrease in MTP activity contributes to HCV core protein-related steatosis, while β -oxidation is unchanged (24), but the mechanism involved is still unclear. This study was the first investigation of the effect of HCV core protein on the expression of fatty acid metabolism-associated molecules in the acute expression mice model.

Hepatic accumulation of TG is principally driven by the following factors: (a) fatty acid overload (28, 29), (b) inhibition of fatty acid β -oxidation (28, 29), (c) decreased secretion of TG-rich very low density lipoprotein (VLDL) (28, 29), (d) increased de novo fatty acid synthesis, (e) decreased transformation to phospholipids, and (f) a combination of these mechanisms.

In the present study, we initially tested the effect of HCV core protein on a human cell line (HepG2). At 24 hr after transfection, the cellular TG level was unchanged, but the expression of several genes that are thought to promote fatty acid consumption (MTP, ACO1, and MDR3) was up-regulated. At 48 hr after transfection, there was either normal gene expression (ACO1) or a decrease in expression (PPAR α , MDR3, and MTP). At 48 hr after transfection, the level of HCV core antigen was still the same as at 24 hr, so it seems possible that HCV core protein may

act to down-regulate these genes over a longer period. To further evaluate the effects of HCV core protein, we performed in vivo experiments using transient expression of HCV core protein in mice. Although fatty change of the liver was not seen histologically, the hepatic TG level was increased by transient HCV core protein expression. In addition, expression of mRNA for all of the molecules investigated, except MTP, was down-regulated by HCV core protein expression. The mechanism involved is not understood at present, but reduced expression of these genes might contribute to hepatic TG accumulation.

CPT is the rate-limiting enzyme for mitochondrial β -oxidation (30), which is the main pathway of fatty acid consumption and ROS production. There was a recent report (20) that localization of HCV core protein in the mitochondria led to the increased production of ROS, decreased mitochondrial membrane permeability, and impairment of mitochondrial function. It remains unclear whether ROS induces fat accumulation or whether the accumulation of fat causes an increase in ROS, as well as whether decreased expression of CPT-1 is the first response to HCV core protein expression or follows other earlier changes. However, HCV core expression seems to contribute to hepatic accumulation of lipids and an increase in ROS in mice, along with reduced expression of various fatty acid metabolism-associated genes. AOX is vital for peroxisomal β -oxidation (30) and it has been reported that AOX knockout mice develop steatohepatitis, up-regulation of CYP4A gene expression, and increased production of ROS (31). We were unable to evaluate CYP4A11 in the present study, but the association of HCV-related steatosis with microsomal ω -oxidation is interesting. Mdr2 (Abcb4) is a member of the Abcb subfamily of adenosine triphosphate-binding cassette (ABC) transporter proteins. Mdr2 Pgp is exclusively localized to the canalicular membrane and controls the secretion of phospholipids into the bile (32). We thought that impaired biliary phospholipid secretion might have a role in HCV-related steatosis, based on the fact that phospholipid-associated fatty acid secretion into bile (about 25 μ mol per day) is substantial in relation to the hepatic amount of triglyceride-associated fatty acids (about 75 μ mol) (33). We found that the expression of MDR3 and Mdr2 was down-regulated, suggesting that reduced expression of these genes could have a causative role in HCV-related steatosis.

Interestingly, down-regulation of Mdr2, AOX, and CPT in the mice was accompanied by down-regulation of PPAR α . In mice, the other three genes are thought to undergo transcriptional regulation by PPAR α (33, 34), so their expression might be down-regulated secondary to the down-regulation of PPAR α . HCV core protein is mainly

localized in the cytosol, but also exists in the nucleus (35, 36), so it is possible that this protein could influence gene transcription. Tsutsumi *et al.* (37) used a luciferase assay to show that transcriptional activation of ACO-1 via PPRE is promoted at 24 hr after HCV core protein expression (23). However, we found down-regulation of target gene expression accompanied by decreased PPAR α expression after 3 days of HCV core protein expression in mice, as well as at 48 hr after transfection of cells. The expression of PPAR α was reported to be under transcriptional regulation by glucocorticoids (38), but the mechanism remains unclear. Accordingly, the mechanism leading to down-regulation of PPAR α after HCV core protein expression is also unclear. The lower expression of PPAR α and the genes it regulates in human hepatocytes than in mouse hepatocytes (39) could be a reason for the lack of an increase in TG and the small decline in gene expression in our cell experiment. Fibrates that bind with PPAR α and increase its activity (although not its expression) might be useful for controlling HCV-related steatosis by increasing the β -oxidation and biliary secretion of fatty acids.

PPAR γ improves insulin resistance and is also reported to improve hepatic fibrosis and nonalcoholic steatohepatitis (40, 41). Because PPAR γ gene expression also showed down-regulation by HCV core protein expression in this study, it may be necessary to examine the role of glucose metabolism, de novo synthesis of fatty acids from glucose, and fatty acid flux through hepatocytes in HCV-related steatosis.

In this study, the increase in TBARS level was found in mice with transient expression of HCV core protein. This suggests that ROS production might be induced by HCV core protein expression, although no mechanistic information for this was provided in this study. It also remains unclear whether intrahepatic fat accumulation enhances ROS production as reflected by an increase in TBARS or, inversely, whether ROS production induces fatty liver change through ROS-associated mitochondrial dysfunction. Certainly, further investigations are needed to clarify this uncertainty, but the fact that HCV core protein expression in mice contributes to the increase in TBARS level may partially characterize the pathogenesis of HCV-related hepatic damage.

In summary, transient expression of HCV core protein in mice down-regulated the expression of various lipid metabolism-associated genes (Mdr2, CPT, and AOX). It also caused down-regulation of PPAR α expression and led to the accumulation of TG and the induction of oxidative stress. These findings may provide some clues to the understanding of HCV-related steatosis and to the induction of ROS production and carcinogenesis by infection with this virus.

REFERENCES

- Alter MJ, Margolis HS, Krawczynski K, Judson FN, Mares A, Alexander WJ, Hu PY, Miller JK, Gerber MA, Sampliner RE, Meeks EL, Beach MJ: The natural history of community-acquired hepatitis C in the United States. *N Engl J Med* 327:1899-1905, 1992
- Seeff LB, Buskell-Bales Z, Wright EC, Durako SJ, Alter HJ, Iber FL, Hollinger FB, Gitnick G, Knodell RG, Perrillo RP, Steevens CE, Hollingworth CG, NHLBI study Group: Long-term mortality after transfusion-associated non-A, non-B hepatitis. *N Engl J Med* 327:1906-1911, 1992
- Seeff LB: Natural history of hepatitis C. *Hepatology* 26:21S-28S, 1997
- Koziel MJ, Dudley D, Wong JT, Dienstag J, Houghton M, Ralston R, Walker BD: Intrahepatic cytotoxic T lymphocytes specific for hepatitis C virus in persons with chronic hepatitis. *J Immunol* 149:3339-3344, 1992
- Cerny A, Chisari FV: Pathogenesis of chronic hepatitis C: immunological features of hepatic injury and viral persistence. *Hepatology* 30:595-601, 1999
- Rubbia-Brandt L, Quadri R, Abid K, Giostra E, Male PJ, Mentha G, Spahr L, Zarski JP, Borisch B, Hadengue A, Negro F: Hepatocyte steatosis is a cytopathic effect of hepatitis C virus genotype 3. *J Hepatol* 33:106-115, 2000
- Scheuer PJ, Davies SE, Dhillon AP: Histopathological aspects of viral hepatitis. *J Viral Hepat* 3:277-283, 1996
- Fujie H, Yotsuyanagi H, Moriya K, Shintani Y, Tsutsumi T, Takayama T, Makuuchi M, Matsuura Y, Miyamura T, Kimura S, Koike K: Steatosis and intrahepatic hepatitis C virus in chronic hepatitis. *J Med Virol* 59:141-145, 1999
- Goodman ZD, Ishak KG: Histopathologic findings in chronic hepatitis C virus infection. *Semin Liver Dis* 15:70-81, 1995
- Barba G, Harper F, Harada T, Kohara M, Goulinet S, Matsuura Y, Eder G, Schaff Z, Chapman MJ, Miyamura T, Brechot C: Hepatitis C virus core protein shows a cytoplasmic localization and associates to cellular lipid storage droplets. *Proc Natl Acad Sci USA* 94:1200-1205, 1997
- Ray RB, Lagging LM, Meyer K, Ray R: Hepatitis C virus core protein cooperates with ras and transforms primary rat embryo fibroblasts to tumorigenic phenotype. *J Virol* 70:4438-4443, 1996
- Ray RB, Meyer K, Ray R: Suppression of apoptotic cell death by hepatitis C virus core protein. *Virology* 226:176-182, 1996
- Zhu N, Khoshnan A, Schneider R, Matsumoto M, Dennert G, Ware C, Lai MM: Hepatitis C virus core protein binds to the cytoplasmic domain of tumor necrosis factor (TNF) receptor 1 and enhances TNF-induced apoptosis. *J Virol* 72:3691-3697, 1998
- Honda M, Kaneko S, Shimazaki T, Matsushita E, Kobayashi K, Ping LH, Zhang HC, Lemon SM: Hepatitis C virus core protein induces apoptosis and impairs cell-cycle regulation in stably transformed Chinese hamster ovary cells. *Hepatology* 31:1351-1359, 2000
- Sakamuro D, Furukawa T, Takegami T, Sakamuro D, Furukawa T, Takegami T: Hepatitis C virus nonstructural protein NS3 transforms NIH 3T3 cells. *J Virol* 69:3893-3896, 1995
- McLauchlan J, Lemberg MK, Hope G, Martoglio B: Intramembrane proteolysis promotes trafficking of hepatitis C virus core protein to lipid droplets. *EMBO J* 21:3980-3988, 2002
- Shi ST, Polyak SJ, Tu H, Taylor DR, Gretch DR, Lai MM: Hepatitis C virus NS5A colocalizes with the core protein on lipid droplets and interacts with apolipoproteins. *Virology* 292:198-210, 2002
- Moriya K, Yotsuyanagi H, Shintani Y, Fujie H, Ishibashi K, Matsuura Y, Miyamura T, Koike K: Hepatitis C virus core protein

- induces hepatic steatosis in transgenic mice. *J Gen Virol* 78:1527–1531, 1997
19. Lerat H, Honda M, Beard MR, Loesch K, Sun J, Yang Y, Okuda M, Gosert R, Xiao SY, Weinman SA, Lemon SM: Steatosis and liver cancer in transgenic mice expressing the structural and nonstructural proteins of hepatitis C virus. *Gastroenterology* 122:352–365, 2002
 20. Okuda M, Li K, Beard MR, Showalter LA, Scholle F, Lemon SM, Weinman SA: Mitochondrial injury, oxidative stress, and antioxidant gene expression are induced by hepatitis C virus core protein. *Gastroenterology* 122:366–375, 2002
 21. Moriya K, Nakagawa K, Santa T, Shintani Y, Fujie H, Miyoshi H, Tsutsumi T, Miyazawa T, Ishibashi K, Horie T, Imai K, Todoroki T, Kimura S, Koike K: Oxidative stress in the absence of inflammation in a mouse model for hepatitis C virus-associated hepatocarcinogenesis. *Cancer Res* 61:4365–4370, 2001
 22. Moriya K, Fujie H, Shintani Y, Yotsuyanagi H, Tsutsumi T, Ishibashi K, Matsuura Y, Kimura S, Miyamura T, Koike K: The core protein of hepatitis C virus induces hepatocellular carcinoma in transgenic mice. *Nat Med* 4:1065–1067, 1998
 23. Sabile A, Perlemuter G, Bono F, Kohara K, Demaugre F, Kohara M, Matsuura Y, Miyamura T, Brechot C, Barba G: Hepatitis C virus core protein binds to apolipoprotein AII and its secretion is modulated by fibrates. *Hepatology* 30:1064–1076, 1999
 24. Perlemuter G, Sabile A, Letteron P, Vona G, Topilco A, Chretien Y, Koike K, Pessayre D, Chapman J, Barba G, Brechot C: Hepatitis C virus core protein inhibits microsomal triglyceride transfer protein activity and very low density lipoprotein secretion: a model of viral-related steatosis. *FASEB J* 16:185–194, 2002
 25. Miyake S, Makimura M, Kanegae Y, Harada S, Sato Y, Takamori K, Tokuda C, Saito I: Efficient generation of recombinant adenoviruses using adenovirus DNA-terminal protein complex and a cosmid bearing the full-length virus genome. *Proc Natl Acad Sci USA* 93:1320–1324, 1996
 26. Kanegae Y, Lee G, Sato Y, Tanaka M, Nakai M, Sakaki T, Sugano S, Saito I: Efficient gene activation in mammalian cells by using recombinant adenovirus expressing site-specific Cre recombinase. *Nucleic Acids Res* 23:3816–3821, 1995
 27. Bligh EG, Dyer WJ: A rapid method of total lipid extraction and purification. *Can J Med Sci* 37:911–917, 1959
 28. Day CP, James OF: Hepatic steatosis: Innocent bystander or guilty party? *Hepatology* 27:1463–1466, 1988
 29. Fong DG, Nehra V, Lindor KD, Buchman AL: Metabolic and nutritional considerations in nonalcoholic fatty liver. *Hepatology* 32:3–10, 2000
 30. Reddy JK: Nonalcoholic steatosis and steatohepatitis. III. Peroxisomal beta-oxidation, PPAR alpha, and steatohepatitis. *Am J Physiol Gastrointest Liver Physiol* 281:G1333–G1339, 2001 (review)
 31. Fan C, Pan J, Chu R, Lee D, Kluckman KD, Usuda N, Singh I, *et al.*: Hepatocellular and hepatic peroxisomal alteration in mice with a disrupted peroxisomal fatty acyl-coenzyme A oxidase gene. *J Biol Chem* 271:24698–24710, 1996
 32. Smit JJ, Schinkel AH: Homozygous disruption of the murine mdr2 P-glycoprotein gene leads to a complete absence of phospholipid from bile and to liver disease. *Cell* 75:451–462, 1993
 33. Kok T, Wolters H, Bloks V, Havinga R, Jansen P, Afaels B, Kuipers F: Induction of hepatic ABC transporter expression is part of the PPAR α -mediated fasting response in the mouse. *Gastroenterology* 124:160–171, 2002
 34. Duplus E, Forest C: Is there a single mechanism for fatty acid regulation of gene transcription? *Biochem Pharmacol* 64:893–901, 2002 (review)
 35. Moriya K, Fujie H, Shintani Y, Yotsuyanagi H, Tsutsumi T, Ishibashi K, Matsuura Y, Kimura S, Miyamura T, Koike K: The core protein of hepatitis C virus induces hepatocellular carcinoma in transgenic mouse. *Nat Med* 4:1065–1067, 1998
 36. Yasui K: The native form and maturation process of hepatitis C virus core protein. *J Virol* 72:6048–6055, 1998
 37. Tsutsumi T, Suzuki T, Shimoiike T, Suzuki R, Moriya K, Shintani Y, Fujie H, Matsuura Y, Koike K, Miyamura T: Interaction of hepatitis C virus core protein with retinoid X receptor α modulates its transcriptional activity. *Hepatology* 35:937–946, 2002
 38. Lemberger T, Saladin R, Vazquez M, Assimakopoulos F, Staelens B, Desvergne B, Wahli W, Auwerx J: Expression of the peroxisome proliferators-activated receptor alpha gene is stimulated by stress and follows a diurnal rhythm. *J Biol Chem* 19:1764–1769, 1996
 39. Hsu M, Savas U, Griffin K, Johnson E: Identification of peroxisome proliferators-responsive human genes by elevated expression of peroxisome proliferators-activated receptor α in HepG2 Cells. *J. Biol. Chem* 276:27950–27958, 2001
 40. Neuschwander-Tetri BA, Brunt EM, Wehmeier KR, Oliver D, Bacon BR: Improved nonalcoholic steatohepatitis after 48 weeks of treatment with the PPAR-gamma ligand rosiglitazone. *Hepatology* 38:1008–1017, 2003
 41. Alter MJ, Margolis HS, Krawczynski K, Judson FN, Mares A, Alexander WJ, Hu PY, Miller JK, Gerber MA, Sampliner RE, Meeks EL, Beach MJ: The natural history of community-acquired hepatitis C in the United States. *N Engl J Med* 327:1899–1905, 1992
 42. Seeff LB, Buskell-Bales Z, Wright EC, Durako SJ, Alter HJ, Iber FL, Hollinger FB, Gitnick G, Knodell RG, Perrillo RP, Steevens CE, Hollingworth CG, NHLBI study Group: Long-term mortality after transfusion-associated non-A, non-B hepatitis. *N Engl J Med* 327:1906–1911, 1992
 43. Seeff LB: Natural history of hepatitis C. *Hepatology* 26:21S–28S, 1997
 44. Kozziel MJ, Dudley D, Wong JT, Dienstag J, Houghton M, Ralston R, Walker BD: Intrahepatic cytotoxic T lymphocytes specific for hepatitis C virus in persons with chronic hepatitis. *J Immunol* 149:3339–3344, 1992
 45. Cerny A, Chisari FV: Pathogenesis of chronic hepatitis C: immunological features of hepatic injury and viral persistence. *Hepatology* 30:595–601, 1999
 46. Rubbia-Brandt L, Quadri R, Abid K, Giostra E, Male PJ, Mentha G, Spahr L, Zarski JP, Borisch B, Hadengue A, Negro F: Hepatocyte steatosis is a cytopathic effect of hepatitis C virus genotype 3. *J Hepatol* 33:106–115, 2000
 47. Scheuer PJ, Davies SE, Dhillon AP: Histopathological aspects of viral hepatitis. *J Viral Hepat* 3:277–283, 1996
 48. Fujie H, Yotsuyanagi H, Moriya K, Shintani Y, Tsutsumi T, Takayama T, Makuuchi M, Matsuura Y, Miyamura T, Kimura S, Koike K: Steatosis and intrahepatic hepatitis C virus in chronic hepatitis. *J Med Virol* 59:141–145, 1999
 49. Goodman ZD, Ishak KG: Histopathologic findings in chronic hepatitis C virus infection. *Semin Liver Dis* 15:70–81, 1995
 50. Barba G, Harper F, Harada T, Kohara M, Goulinet S, Matsuura Y, Eder G, Schaff Z, Chapman MJ, Miyamura T, Brechot C: Hepatitis C virus core protein shows a cytoplasmic localization and associates to cellular lipid storage droplets. *Proc Natl Acad Sci USA* 94:1200–1205, 1997
 51. Ray RB, Lagging LM, Meyer K, Ray R: Hepatitis C virus core protein cooperates with ras and transforms primary rat embryo fibroblasts to tumorigenic phenotype. *J Virol* 70:4438–4443, 1996
 52. Ray RB, Meyer K, Ray R: Suppression of apoptotic cell death by hepatitis C virus core protein. *Virology* 226:176–182, 1996

53. Zhu N, Khoshnan A, Schneider R, Matsumoto M, Dennert G, Ware C, Lai MM: Hepatitis C virus core protein binds to the cytoplasmic domain of tumor necrosis factor (TNF) receptor 1 and enhances TNF-induced apoptosis. *J Virol* 72:3691–3697, 1998
54. Honda M, Kaneko S, Shimazaki T, Matsushita E, Kobayashi K, Ping LH, Zhang HC, Lemon SM: Hepatitis C virus core protein induces apoptosis and impairs cell-cycle regulation in stably transformed Chinese hamster ovary cells. *Hepatology* 31:1351–1359, 2000
55. Sakamuro D, Furukawa T, Takegami T, Sakamuro D, Furukawa T, Takegami T: Hepatitis C virus nonstructural protein NS3 transforms NIH 3T3 cells. *J Virol* 69:3893–3896, 1995
56. McLauchlan J, Lemberg MK, Hope G, Martoglio B: Intramembrane proteolysis promotes trafficking of hepatitis C virus core protein to lipid droplets. *EMBO J* 21:3980–3988, 2002
57. Shi ST, Polyak SJ, Tu H, Taylor DR, Gretch DR, Lai MM: Hepatitis C virus NS5A colocalizes with the core protein on lipid droplets and interacts with apolipoproteins. *Virology* 292:198–210, 2002
58. Moriya K, Yotsuyanagi H, Shintani Y, Fujie H, Ishibashi K, Matsuura Y, Miyamura T, Koike K: Hepatitis C virus core protein induces hepatic steatosis in transgenic mice. *J Gen Virol* 78:1527–1531, 1997
59. Lerat H, Honda M, Beard MR, Loesch K, Sun J, Yang Y, Okuda M, Gosert R, Xiao SY, Weinman SA, Lemon SM: Steatosis and liver cancer in transgenic mice expressing the structural and nonstructural proteins of hepatitis C virus. *Gastroenterology* 122:352–365, 2002
60. Okuda M, Li K, Beard MR, Showalter LA, Scholle F, Lemon SM, Weinman SA: Mitochondrial injury, oxidative stress, and antioxidant gene expression are induced by hepatitis C virus core protein. *Gastroenterology* 122:366–375, 2002
61. Moriya K, Nakagawa K, Santa T, Shintani Y, Fujie H, Miyoshi H, Tsutsumi T, Miyazawa T, Ishibashi K, Horie T, Imai K, Todoroki T, Kimura S, Koike K: Oxidative stress in the absence of inflammation in a mouse model for hepatitis C virus-associated hepatocarcinogenesis. *Cancer Res* 61:4365–4370, 2001
62. Moriya K, Fujie H, Shintani Y, Yotsuyanagi H, Tsutsumi T, Ishibashi K, Matsuura Y, Kimura S, Miyamura T, Koike K: The core protein of hepatitis C virus induces hepatocellular carcinoma in transgenic mice. *Nat Med* 4:1065–1067, 1998
63. Sabile A, Perlemuter G, Bono F, Kohara K, Demaugre F, Kohara M, Matsuura Y, Miyamura T, Brechot C, Barba G: Hepatitis C virus core protein binds to apolipoprotein AII and its secretion is modulated by fibrates. *Hepatology* 30:1064–1076, 1999
64. Perlemuter G, Sabile A, Letteron P, Vona G, Topilco A, Chretien Y, Koike K, Pessayre D, Chapman J, Barba G, Brechot C: Hepatitis C virus core protein inhibits microsomal triglyceride transfer protein activity and very low density lipoprotein secretion: a model of viral-related steatosis. *FASEB J* 16:185–194, 2002
65. Miyake S, Makimura M, Kanegae Y, Harada S, Sato Y, Takamori K, Tokuda C, Saito I: Efficient generation of recombinant adenoviruses using adenovirus DNA-terminal protein complex and a cosmid bearing the full-length virus genome. *Proc Natl Acad Sci USA* 93:1320–1324, 1996
66. Kanegae Y, Lee G, Sato Y, Tanaka M, Nakai M, Sakaki T, Sugano S, Saito I: Efficient gene activation in mammalian cells by using recombinant adenovirus expressing site-specific Cre recombinase. *Nucleic Acids Res* 23:3816–3821, 1995
67. Bligh EG, Dyer WJ: A rapid method of total lipid extraction and purification. *Can J Med Sci* 37:911–917, 1959
68. Day CP, James OF: Hepatic steatosis: Innocent bystander or guilty party? *Hepatology* 27:1463–1466, 1988
69. Fong DG, Nehra V, Lindor KD, Buchman AL: Metabolic and nutritional considerations in nonalcoholic fatty liver. *Hepatology* 32:3–10, 2000
70. Reddy JK: Nonalcoholic steatosis and steatohepatitis. III. Peroxisomal beta-oxidation, PPAR alpha, and steatohepatitis. *Am J Physiol Gastrointest Liver Physiol* 281:G1333–G1339, 2001 (review)
71. Fan C, Pan J, Chu R, Lee D, Kluckman KD, Usuda N, Singh I, *et al.*: Hepatocellular and hepatic peroxisomal alternation in mice with a disrupted peroxisomal fatty acyl-coenzyme A oxidase gene. *J Biol Chem* 271:24698–24710, 1996
72. Smit JJ, Schinkel AH: Homozygous disruption of the murine mdr2 P-glycoprotein gene leads to a complete absence of phospholipid from bile and to liver disease. *Cell* 75:451–462, 1993
73. Kok T, Wolters H, Bloks V, Havinga R, Jansen P, Ataels B, Kuipers F: Induction of hepatic ABC transporter expression is part of the PPAR α -mediated fasting response in the mouse. *Gastroenterology* 124:160–171, 2002
74. Duplus E, Forest C: Is there a single mechanism for fatty acid regulation of gene transcription? *Biochem Pharmacol* 64:893–901, 2002 (review)
75. Moriya K, Fujie H, Shintani Y, Yotsuyanagi H, Tsutsumi T, Ishibashi K, Matsuura Y, Kimura S, Miyamura T, Koike K: The core protein of hepatitis C virus induces hepatocellular carcinoma in transgenic mouse. *Nat Med* 4:1065–1067, 1998
76. Yasui K: The native form and maturation process of hepatitis C virus core protein. *J Virol* 72:6048–6055, 1998
77. Tsutsumi T, Suzuki T, Shimoike T, Suzuki R, Moriya K, Shintani Y, Fujie H, Matsuura Y, Koike K, Miyamura T: Interaction of hepatitis C virus core protein with retinoid X receptor α modulates its transcriptional activity. *Hepatology* 35:937–946, 2002
78. Lemberger T, Saladin R, Vazquez M, Assimakopoulos F, Staels B, Desvergne B, Wahli W, Auwerx J: Expression of the peroxisome proliferators-activated receptor alpha gene is stimulated by stress and follows a diurnal rhythm. *J Biol Chem* 19:1764–1769, 1996
79. Hsu M, Savas U, Griffin K, Johnson E: Identification of peroxisome proliferators-responsive human genes by elevated expression of peroxisome proliferators-activated receptor α in HepG2 Cells. *J Biol Chem* 276:27950–27958, 2001
80. Neuschwander-Tetri BA, Brunt EM, Wehmeier KR, Oliver D, Bacon BR: Improved nonalcoholic steatohepatitis after 48 weeks of treatment with the PPAR-gamma ligand rosiglitazone. *Hepatology* 38:008–1017, 2003
81. Promrat K, Lutchman G, Uwaifo GI, Freedman RJ, Soza A, Heller T, Doo E, Ghany M, Premkumar A, Park Y, Liang TJ, Yanovski JA, Kleiner DE, Hoofnagle JH: A pilot study of pioglitazone treatment for nonalcoholic steatohepatitis. *Hepatology* 39:188–196, 2004

G to A Hypermutation of Hepatitis B Virus

Chiemi Noguchi,^{1,2} Hiromi Ishino,¹ Masataka Tsuge,¹ Yoshifumi Fujimoto,³ Michio Imamura,^{1,2} Shoichi Takahashi,^{1,2} and Kazuaki Chayama^{1,2,3}

G to A hypermutation of the human immunodeficiency virus type 1 (HIV-1) is induced by a deaminase APOBEC3G and is related to host antiviral defense. APOBEC3G has also been found to reduce the replication of HIV-1 by an unknown mechanism. This enzyme also reduces the production of hepatitis B virus, although the mechanism for this action has not been clearly elucidated. The hypermutated hepatitis B virus (HBV) is rarely found in usual sequencing analyses. Using peptide nucleic acid mediated by polymerase chain reaction clamping, we detected the hypermutated HBV DNA in 1 of 8 patients with acute HBV infection and 4 of 10 with chronic HBV infection. In the latter group, hypermutated genomes were found only in eAb-positive patients. As much as 72.5% of G residues were mutated in the hypermutated clones. G to A substitutions were predominant in almost all clones sequenced compared with other substitutions. G to A mutated viral genomes also were found in HepG2-derived cell lines that continuously produced HBV into the supernatant. Both alpha and gamma interferon reduced virus production in these cell lines, but they did not alter the frequency of the hypermutation. Transcripts of APOBEC3G, as well as some other deaminases, were found in these cell lines. **In conclusion**, our results show that part of the minus strand DNA of HBV is hypermutated both *in vitro* (HepG2 cell lines) and *in vivo*. The role and mechanism of hypermutation in reducing HBV replication should be further investigated to understand the anti-HBV defense system. (HEPATOLOGY 2005;41:626-633.)

Hepatitis B virus (HBV) is a small enveloped DNA virus that replicates in hepatocytes in a noncytolytic manner. Chronic infection with the virus often leads to chronic hepatitis and liver cirrhosis. Hepatocellular carcinoma arises in chronic carriers at a higher frequency than noninfected individuals.¹⁻⁴

The replication cycle of the HBV includes pregenome RNA synthesis and reverse transcription, resulting in the production of the minus strand DNA, which serves as a template of the plus strand DNA.⁵ The life cycle of this virus resembles that of the human immunodeficiency virus 1 (HIV-1), which also replicates through reverse transcription.⁶

Recent reports showed that a cytosine deaminase APOBEC3G (apolipoprotein B mRNA-editing enzyme, catalytic polypeptide-like 3G), which is packaged in HIV-1 virions, induces G to A hypermutation to a nascent reverse transcript of HIV-1, which contributes in part to the innate antiviral activity.⁷⁻¹⁰ The antiviral activity of APOBEC3G is species specific^{11,12} and may represent the different actions of the protein.^{13,14} The virion infectivity factor encoded by lentivirus genomes associates with APOBEC3G to prevent the enzyme from being packaged into virions and triggers its proteasomal degradation.¹⁵⁻¹⁸ The negative strand DNA of the HBV might be a target of such antiviral deaminase activity. In fact, naturally occurring HBV genomes bearing the hallmarks of retroviral G to A hypermutation have been reported in clones obtained from 2 HBV carriers.¹⁹ Both of these clones represented subgenomes arising from reverse transcrip-

Abbreviations: HBV, hepatitis B virus; HIV-1, human immunodeficiency virus type 1; APOBEC3G, apolipoprotein B mRNA-editing enzyme, catalytic polypeptide-like 3G; HBsAg, hepatitis B surface antigen; HBeAg, hepatitis B early antigen; PCR, polymerase chain reaction; PNA, peptide nucleic acid.

From the ¹Department of Medicine and Molecular Science, Division of Frontier Medical Science, Programs for Biomedical Research, Graduate School of Biomedical Sciences, Hiroshima University, Hiroshima, Japan; ²Hiroshima Liver Research Center, Hiroshima University, Hiroshima, Japan; and ³Laboratory for Liver Diseases, SNP Research Center, Institute of Physical and Chemical Research (RIKEN), Yokohama, Japan.

Received August 27, 2004; accepted December 2, 2004.

Supported in part by a Grant-in-Aid from the Ministry of Education, Culture, Sports, Science and Technology, Japan.

Address reprint requests to: Kazuaki Chayama, M.D., Department of Medicine and Molecular Science, Division of Frontier Medical Science, Programs for Biomedical Research, Graduate School of Biomedical Sciences, Hiroshima University, 1-2-3 Kasumi, Minami-ku, Hiroshima 734-8551, Japan. E-mail: chayama@hiroshima-u.ac.jp; fax: (81) 82-255-6220.

Copyright © 2005 by the American Association for the Study of Liver Diseases.

Published online in Wiley InterScience (www.interscience.wiley.com).

DOI 10.1002/hep.20580

Conflict of interest: Nothing to report.

tion of packaged spliced mRNA. However, such hypermutated genomes have otherwise never been reported, nor deposited in DNA databases. Moreover, whether such hypermutated sequences are generated in liver cells or in leukocytes is unknown.

Inhibition of HBV replication by APOBEC3G was observed recently in a transient transfection system.²⁰ However, no induction of hypermutations to the HBV genome was observed. Instead, prevention of pre-genome RNA packaging was observed.

The aims of the current study were to determine the frequency of viral genomes with G to A substitutions in HBV carriers and patients with acute HBV infection, and to determine whether the hypermutated sequences are generated in hepatic cell lines. We identified such hypermutated viral genomes in 5 of 18 HBV carriers and patients with acute HBV infection and the expression of known deaminases that are potentially responsible for the hypermutation in cultured hepatoma cell lines.

Materials and Methods

Serum Samples. Serum samples from 18 adult Japanese patients with HBV infection were studied. At the time of the study, 8 of these patients had acute HBV infection and tested positive for immunoglobulin M anti-hepatitis B core antibody. The remaining 10 patients were chronic carriers. All serum samples were stored at -80°C until examined. All patients were negative for serum markers of both hepatitis C virus and HIV-1 infection, and none was on antiviral treatment.

Serological Markers of HBV Infection. Hepatitis B surface antigen (HBsAg) was detected by enzyme immunoassay (Roche Diagnostics, Basel, Switzerland), and hepatitis B early antigen (HBeAg) as well as anti-HBe were detected by radioimmunoassay (Abbott Diagnostics, Abbott Park, IL). HBV DNA was determined by transcription-mediated amplification and hybridization-protection assay (Chugai Diagnostics, Tokyo, Japan), and the results were expressed as log genome equivalents per milliliter. The lower detection limit of this assay is 3.7 log genome equivalents/mL (equivalent to 5,000 copies/mL). The antibody against hepatitis C virus was tested for by the third-generation enzyme immunoassay (Roche Diagnostics).

Analysis of HBV DNA in Cell Lines That Stably Produce HBV. Two cell lines known to produce wild-type HBV and one cell line known to produce lamivudine-resistant HBV (with mutations of L528M and M552V) were created by transfecting 1.4 genome length sequences of HBV to HepG2 cell lines. These cell lines produced HBV that showed a similar sedimentation in

sucrose density gradient centrifugation to HBV extracted from the serum of carriers (M. Tsuge et al., manuscript in preparation) and could infect human hepatocyte chimeric mice (manuscript in preparation). These cell lines were grown in Dulbecco's modified Eagle's medium supplemented with 10% (vol/vol) fetal bovine serum at 37°C and 5% CO_2 . Cells were seeded to semiconfluence in 6-well tissue culture plates and then treated with media containing interferon alpha or gamma. After 3 days of interferon treatment, the cells were harvested and lysed with 250 μL lysis buffer (10 mmol/L Tris-HCl [pH 7.4], 140 mmol/L NaCl, 0.5% [vol/vol] NP-40) followed by centrifugation for 2 minutes at 15,000g. Replicative intermediate of the HBV was immunoprecipitated and subjected to Southern blot analysis and quantitative analysis by light cycler. The effect of lamivudine was analyzed similarly, except that cells were harvested after 5 days of treatment.

Detection of Hypermutated Clones by Polymerase Chain Reaction With PNA Clamping, Cloning, and Sequencing. HBV DNA was extracted from 100 μL serum or culture supernatant by SMITEST (Genome Science Laboratories, Tokyo, Japan) and was dissolved in 20 μL H_2O . The first round of polymerase chain reaction (PCR) was performed with an outer primer set (PLF1 and BR112 [Table 1]) and a second-round PCR with an inner primer set (PLF2 and PLR2 [Table 1]). The peptic nucleic acid (PNA) oligonucleotide, initially designed to detect lamivudine-resistant variant genome,²¹ was an 18-mer (PNA 552 [Table 1]) that exactly matched the 18-nucleotide sequence of the original YMDD sequence of DNA polymerase/reverse transcriptase, which contained GG and TG sequences (AGT TAT ATG GAT GAT GTG). The PCR with PNA clamping was performed in a total volume of 25 μL , consisting of a reaction buffer (100 mmol/L Tris-HCl [pH 8.3], 50 mmol/L KCl and 15 mmol/L MgCl_2), 0.2 mmol/L each of dNTPs, 1 μL of the DNA solution, 12.5 pmol each primer, 150 pmol PNA 552, and 1 unit of Taq DNA polymerase (Gene Taq, Wako Pure Chemicals, Tokyo, Japan) together with 0.2 μg anti-Taq high (Toyobo Co., Osaka, Japan). The amplification conditions included an initial denaturation at 95°C for 4 minutes and 25 cycles of amplification (denaturation at 95°C for 45 seconds, PNA annealing at 73°C for 2 minutes, annealing and extension of primer at 63°C for 50 seconds), followed by a final extension at 63°C for 7 minutes. Part of the X gene was amplified with an outer primer pair (HBV1 and HBV2) and an inner primer (PLF2 and HBV2) (Table 1) for the first- and second-round amplifications, respectively. The amplification for the first-round PCR included initial denaturation at 95°C for 4 minutes and 25 cycles of amplification (denatur-

Table 1. Oligonucleotides and PNAs Used in the Current Study

Primer	Sequence
HBV amplification	
PLF1	5'-GGT ATG TTG CCC GTT TGT CC-3'
BR112	5'-TTC CGT CGA CAT ATC CCA T-3'
PLF2	5'-CCT ATG GGA GTG GGC CTC AG-3'
PLR2	5'-CCA ATT ACA TAT CCC ATG AAG TTA AGG GA-3'
HBV1	5'-CCG GAA AGC TTG AGC TCT TCT TTT TCA CCT CTG CCT AAT CA-3'
HBV2	5'-CCG GAA AGC TTG AGC TCT TCA AAA AGT TGC ATG GTG CTG G-3'
BR109	5'-AAG GGA GTA GCC CCA ACG TT-3'
PNA	
PNA552	H2N-CAC ATC ATC CAT ATA ACT-CON2H
PNA552V	H2N-CAC ATC ATC CAC ATA ACT-CON2H
Amplification of mRNAs of deaminases	
APO1a	5'-CAG AGC ACC ATG ACT TCT-3'
APO1d	5'-ATT GTG GCC AGT GAG CIT CA-3'
APO2a	5'-AGA AGG AAG AGG CTG CTG TG-3'
APO2b	5'-AGA ACG GCT GCC TGC CAA CT-3'
APO2c	5'-GAA GGC TGG CAG GAT GGT GT-3'
APO2d	5'-CAG GTG ACA TTG TAC CGC AG-3'
APO3Aa	5'-TCT TAA CAC CAC GCC TTG AG-3'
APO3Ad	5'-GAA GAT GCG CAG TCT CAC GT-3'
APO3Ba	5'-AGA GCG GGA CAG GGA CAA GC-3'
APO3Bb	5'-GCG TAT CTA AGA GGC TGA AC-3'
APO3Bd	5'-CGA AGG ACC AAA GGG TCA TT-3'
APO3Be	5'-ACA AGT AGG TCT GGC GCC GT-3'
APO3Ca	5'-AGG ACG CTG TAA GCA GGA AG-3'
APO3Cb	5'-CCG ATG AAG GCA ATG TAT GG-3'
APO3Cc	5'-GTC GTC GCA GAA CCA AGA GA-3'
APO3Cd	5'-GAT GTG TAC CAG GTG ACC TG-3'
APO3Da	5'-CTG GGA CAA GCG TAT CTA AG-3'
APO3Dd	5'-AGT CTG AGA TGA AGA GGT GG-3'
APO3Fa	5'-CIT GGG TCC TGC CGC ACA GA-3'
APO3Fd	5'-TCA TCC TTG GCC GGC TAG TC-3'
APO3Ga	5'-GAC TAG CCG GCC AAG GAT GA-3'
APO3Gb	5'-CAC AGT GGA GCG AAT GTA TC-3'
APO3Gc	5'-GTT CGG AAT ACA CCT GGC CT-3'
APO3Gd	5'-ACT CCT GGT CAC GAT GCA GC-3'

ation at 95°C for 45 seconds, PNA annealing at 73°C for 2 minutes, primer annealing at 60°C for 1 minute, and extension of primer at 63°C for 4 minutes), followed by the final extension at 63°C for 7 minutes. The second-round amplification was performed under the same conditions without a primer extension for 3 minutes. The estimated error rate of the Taq DNA polymerase was 1.76×10^{-5} per site in amplifying approximately 10^2 copies of plasmid under the same conditions as described previously and cloning and sequencing.²¹ Products (1 μ L each) of the second-round of PNA PCR were subjected to PCR with primers PLF2 and BR109 for 35 cycles (94°C, 1 minute; 58°C, 1 minute; 72°C, 1.5 minutes) after initial denaturation at 94°C for 4 minutes and followed by the final extension at 72°C for 7 minutes. Amplicons were purified by electrophoresis on 2% (wt/vol) agarose gel and cloned into pGEM-T Easy Vector (Promega, Madison, WI) with the standard method, and then transformed

into *Escherichia coli* JM 109 (Takara Shuzo Co., Otsu, Japan). Sequencing was performed in the ABI PLISM TM 310NT Genetic analyzer (Applied Biosystems, Tokyo, Japan) with Big Dye terminator version 3.0 Cycle Sequencing Ready Reaction kit (Applied Biosystems). Ten independent clones from each serum sample of patients or supernatant of cell cultures were sequenced for analysis and compared for nucleotide sequences obtained by direct sequencing of PCR products. Hypermutation was defined as clones with a statistically significant number of G to A substitutions.

Sequence Analysis. Nucleotide sequences were aligned and parameters of hypermutation were evaluated with Hypermut Program Package²² (<http://www.hiv.lanl.gov/HYPERMUT/hypermut.html>). We used nucleotide sequences obtained by direct sequencing as reference sequences and tentatively labeled clones with a statistically significant ($P < .05$ by Fisher's exact test) number of G to A substitutions as "hypermutated."

Detection of mRNA of Known Deaminases by Reverse Transcription and PCR. Total RNA was extracted from HepG2 cell lines by using cell-to-cDNAII kit (Ambion, Austin, TX). The extracted RNA was reverse transcribed with random primer and M-MLV reverse transcriptase (ReverTra Ace, TOYOBO, Osaka, Japan) at 42°C for 60 minutes according to the instructions provided by the manufacturer. Synthesized cDNAs were used to detect mRNAs of known deaminases using primers listed in Table 1. Each of these primers was carefully designed to amplify only the target member of the APOBEC families. Amplification of specific deaminases was confirmed by amplifying each deaminase cDNA by using cDNAs obtained from organs reported to be positive for the expression of each deaminase. The amplicons were analyzed in 2% agarose gel, and the nucleotide sequences were confirmed by direct sequencing.

Results

Frequent Detection of G to A Substituted HBV Genomes by PCR With PNA Clamping in Patients With Acute or Chronic Hepatitis B Virus Infection. Using PCR with PNA clamping, clones with multiple G to A substitutions were found (Table 2). In contrast, only small numbers of other substitutions were identified in these clones. A hypermutated genome of HBV was found in 1 of 8 patients with acute HBV infection and 4 of 10 patients with chronic HBV infection (Table 2). We cloned and sequenced more than 20 clones without PNA and found no hypermutated clones. Among patients with chronic HBV infection, hypermutated clones were identified only in eAb-positive patients (Table 2). Figure 1

Table 2. Nucleotide Substitutions of Clones Amplified by PCR With PNA Clamping and Clinical Features of Patients With Acute and Chronic Hepatitis B Virus Infections

Patient	No. of Substitutions*		No. of Clones†	Pre-core‡	CP§	eAg	eAb	HBV DNA	ALT
	G to A	Other							
A-1	27	3	B (1)	G	A/G	42	0	5.1	2,517
A-2	13	4	8	G	A/G	7.8	88	6.1	3,778
A-3	12	2	5	A/G	A/G	190	0	<3.7	1,417
A-4	11	0	4	G	A/G	58.3	0	4.5	2,550
A-5	11	3	9	G	A/G	170	0	8.3	175
A-6	7	7	9	A/G	Mixed	260	0	7.8	28
A-7	1	2	4	G	Mixed	0.1	99.4	4.1	2,295
A-8	1	1	3	A	T/A	0.7	91	7.1	6,183
C-1	152	2	10 (10)	A	T/A	0.3	100	5.5	394
C-2	44	12	9 (4)	A/G	T/A	18.2	73.4	6.2	340
C-3	30	4	10 (1)	A/G	T/A	0.3	97	7.3	53
C-4	23	1	3	G	A/G	140	0	5.9	2,770
C-5	22	1	8 (1)	A	T/A	0.4	95	6.5	105
C-6	19	9	9	A/G	Mixed	200	0	8.2	113
C-7	18	5	7	G	T/A	170	0	6.6	31
C-8	17	1	7	G	A/G	200	0	7.7	92
C-9	12	4	7	G	T/A	180	0	>8.8	56
C-10	6	4	7	A	A/G	2.5	95	8.3	267

*Total number of nucleotide substitutions in 10 clones compared with sequences obtained by direct sequencing.

†Number of different clones of 10 clones sequenced. Figures in parentheses represent the number of clones with hypermutation (those with a statistically significant number of G to A substitutions).

‡Nucleotide sequence of codon 28 of pre-core protein (nucleotide 1896).

§Nucleotide sequence of basic core promoter (nucleotides 1762 and 1764). Mixed represents mixture of A/G and T/A.

illustrates hypermutations found in an eAb-positive patient with chronic HBV infection (C-1 in Table 2). As much as 72.5% (29 of 40) of G residues were mutated in such hypermutated clones. Hypermutation was found in both the envelope/polymerase region (Fig. 1A) and x region (Fig. 1B) of HBV genome obtained from this patient. Preference of G to A mutation was similar with those reported in HIV-1; that is, G residues in GA sequences were the most frequently hypermutated (Fig. 2).

In contrast, the G residues in CxG context were less frequently substituted (Fig. 2). Numerous G to A nucleotide substitutions were identified in clones lacking a statistically significant number of G to A hypermutations (Table 2). The number of such substitutions was apparently greater than "other substitutions" (Table 2). There was no relationship between the degree of hypermutation and serum alanine aminotransferase concentration or HBV DNA level (Table 2).

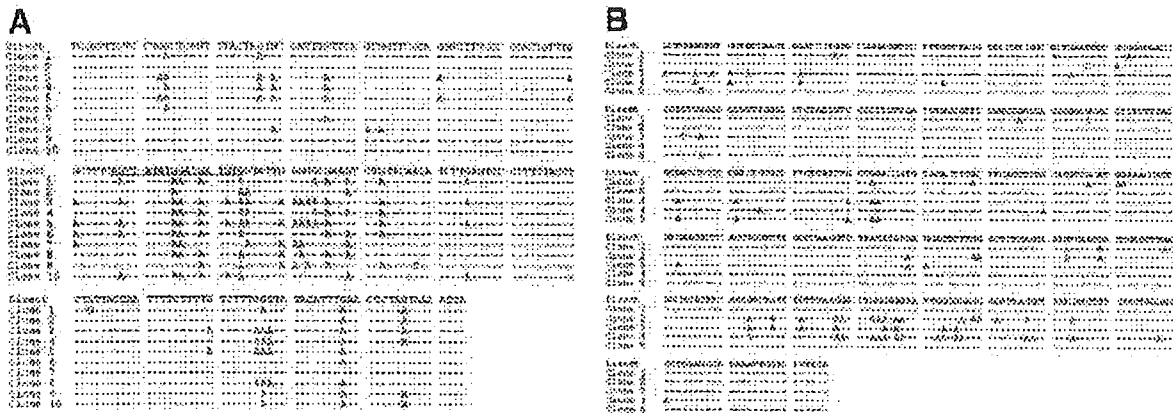


Fig. 1. G to A hypermutations detected in sequences of HBV DNA in sera extracted from an HBe antibody-positive HBV carrier (Patient C-1, Table 2) by PCR with PNA clamping. (A) DNA sequence alignment in the HBs antigen/polymerase region of the HBV. The nucleotide sequences that were obtained by direct sequencing were used as a reference sequence (top line). The target sequence of PNA annealing is underlined. (B) DNA sequence alignment in the x region of the HBV.

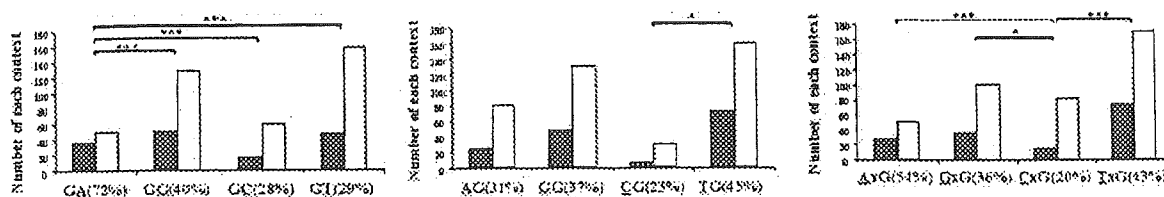


Fig. 2. Preferred nucleotide contexts of G to A hypermutation in 10 clones from patient C-1 (Table 2). The preferred nucleotide letter one letter after (left), one letter before (middle), and two places before (right, x = any) the target G residue. **Open bars:** number of occurrences of each context in the sequence analyzed. **Gray bars:** number of G residues mutated to A. The percentage in parentheses represents the rate of mutated G residues. * $P < .05$, *** $< .001$ (Fisher's exact test or chi-square test).

G to A Hypermutation in HBV-Producing Cell Lines. We established HepG2 cell lines that continuously produced HBV into the medium and examined the frequency of hypermutation. Hypermutated clones were identified in one of these cell lines (Table 3 and Fig. 3). The preference of G to A mutation was similar to that found in serum samples obtained from patients (data not shown). Various levels of HBsAg, HBeAg, and HBV DNA were released into the medium from these cells (Table 3). No relationship was found between the frequency of the hypermutated genome and intracellular intermediates of HBV DNA and HBsAg and HBeAg levels (Table 3). Figure 4 shows replicative intermediates of the HBV produced in these cell lines detected by Southern blot analysis (Fig. 4). No noticeable difference was observed between a cell line with hypermutated genomes and those without hypermutated genomes (lanes 1 and 2 in Fig. 4).

G to A Hypermutation During Antiviral Treatment. We treated the cell lines with alpha and gamma interferon and lamivudine. Both interferons reduced HBV DNA production from these cells in a dose-dependent manner (Fig. 5). The frequency of G to A hypermutation did not increase in those treated cell lines (Fig. 6), suggesting that G to A hypermutation is not responsible

for antiviral defense through these interferons. Treatment of a cell line with lamivudine resulted in marked reductions in the production of HBV in the supernatant as well as intracellular viral intermediates (Fig. 7) and completely abolished identification of G to A substitution (Fig. 6). A similar reduction of detection of hypermutated clones was observed in serum samples obtained from patients who were treated with lamivudine (data not shown).

Expression of Deaminases in HepG2 Cell Lines. We examined the expression of known deaminases to see whether any such enzymes are active in HepG2 cells. As shown in Fig. 8, mRNA expression of 5 of 8 of these deaminases was detected, although the expression level of some deaminases was very low. mRNA of Apobec3G, a key enzyme for the hypermutation of HIV-1, was expressed in HepG2 cells, but the cDNA of this enzyme was only found by nested PCR. The expression level of the mRNA was similar in HBV-producing cells with various levels of hypermutations of HBV as well as parent HepG2 cells (detected by only nested PCR).

Discussion

In this study, we detected the mutated HBV genome in some patients by using PCR with PNA clamping. PNA is a DNA analog in which the ribose-phosphodiester backbone of DNA has been replaced by *N*-(2-aminoethyl) glycine linkages.²³ The PNA anneals strongly to DNA like a complementary DNA, but with higher affinity.²³ The annealing of the PNA to the target sequence thus prevents amplification of the target DNA in the PCR. In our previous study,²¹ we attempted to block the amplification of lamivudine-sensitive wild-type YMDD motif strain and detected a very small amount (1/10,000) of YMDD motif mutant. Because the target sequence of this system contained many Gs with GA and GG (AGT TAT ATG GAT GAT GTG), we assumed that we could detect very rare hypermutated genomes.

Because we did not detect any hypermutated sequence without PNA, we assumed that the rate of the hypermutated genome is very low. This low frequency of hyper-

Table 3. Nucleotide Substitutions of Clones Amplified by PCR With PNA Clamping in Three Cell Lines That Produce the Hepatitis B Virus

Cell Line	No. of Substitutions*		No. of Clones†	eAg	HBs Ag	HBV DNA
	G to A	Other				
Cell line 1	102	0	10 (7)	17	4.7	5.2
Cell line 2	19	0	7	10	4.9	4.6
Cell line 3	21	1	6	14	2.8	4.6

*Total number of nucleotide substitutions in ten clones compared with sequences of the transfected clone.

†Number of different clones of 10 clones sequenced. The figure in parentheses represents the number of clones with hypermutation (those with a statistically significant number of G to A substitutions). Codon 28 of the pre-core gene of the transfected clone was wild (Trp), and nucleotides 1762/1764 were T/A.

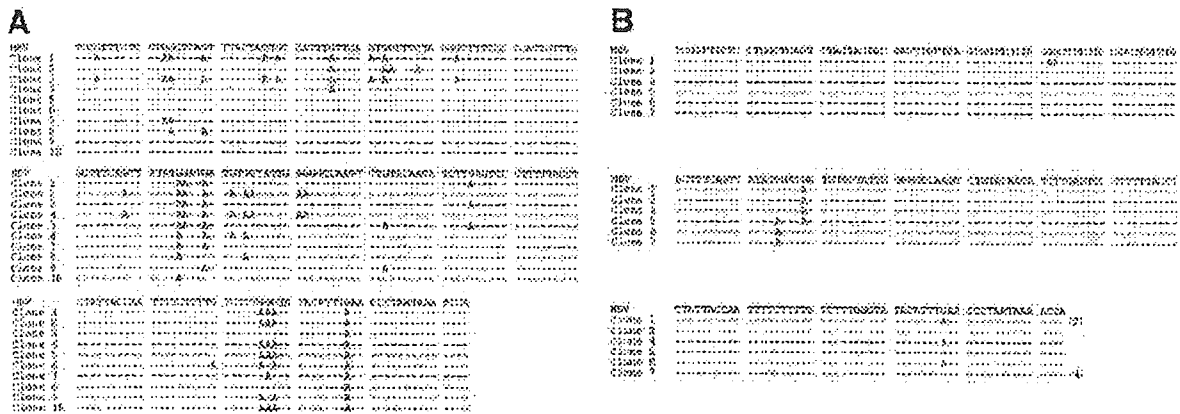


Fig. 3. G to A hypermutations detected in sequences of the HBV DNA (produced by HBV DNA-transfected cell lines to the supernatants). The nucleotide sequences of the transfected clone were used as a reference sequence (top line). DNA sequence alignments in the HBs antigen/polymerase region of cell line 1 (A) and cell line 2 (B) of the HBV. Numbers in parentheses are numbers of clones.

mutated genomes accounts for the lack of reports of such sequences with only one exception until recently,¹⁹ in which the presence of two clones of hypermutated sequences in spliced genomes was reported. One may assume that the rare hypermutated genome might be produced in peripheral blood mononuclear cells because the HBV genome was previously found in such cells.²⁴⁻²⁸ However, we showed that these genomes are found in HBV-transfected cell lines. Our results clearly demonstrate that hypermutation actually occurs in hepatocytes. The reason(s) for such a low frequency of hypermutation

is not clear. The low expression level of deaminases in hepatocytes might account for the low frequency. In fact, we observed a very low expression level of APOVEC3G (transcripts was only detected by nested PCR [Fig. 8]) in HepG2 cell lines.

Recently, Turelli et al.^{20,29} suggested that overexpression of APOBEC3G inhibits the replication of HBV by preventing encapsidation of the virus. However, they did not observe an increase in G to A hypermutation. In contrast, Rosler et al.³⁰ reported that G to A substitutions significantly increased in HepG2 cells when co-transfected with APOBEC3G cDNA. They found only 50 G to A substitutions by cloning 223 clones,³⁰ suggesting that the frequency of G to A substitutions is rare despite overexpression of APOBEC3G. Our preliminary data suggest that overexpression of APOBEC3G does not produce a

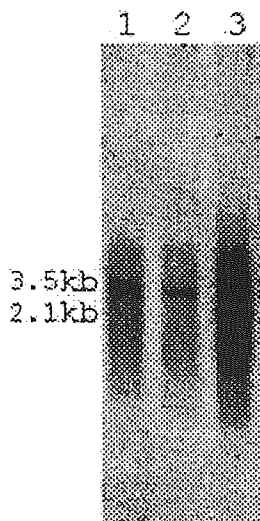


Fig. 4. Southern blot analysis of the HBV DNA extracted from cell lines that stably produce HBV into the supernatant. Two YMDD wild-type virus sequences (lanes 1 and 2) and one YVDD mutant virus sequence (lane 3) were transfected into the HepG2 cell line.

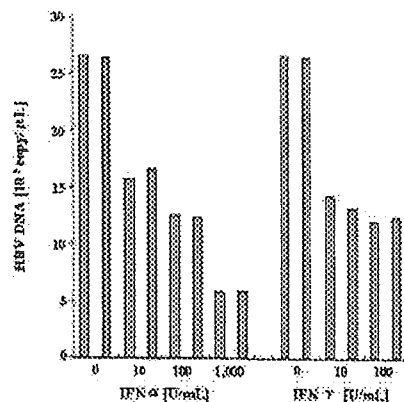


Fig. 5. Effects of interferon alpha and gamma on production of HBV DNA by cell line 1. Experiments were performed in duplicate with increasing amounts of each interferon.

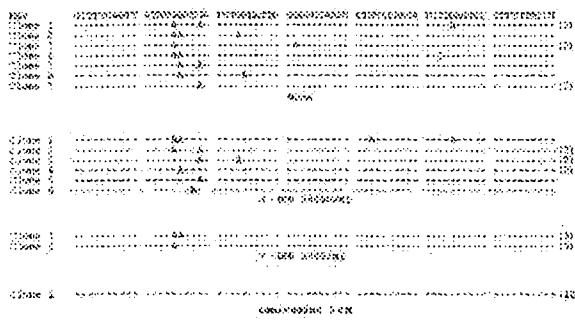


Fig. 6. Nucleotide sequence substitutions around YMDD motif of reverse transcriptase detected by PCR with PNA clamping after treating a HepG2 cell line (cell line 2 in Table 3). The nucleotide sequence of the transfected clone was used as a reference sequence (top line). Cells were treated with interferons and lamivudine as shown in Figs. 5 and 7, respectively.

noticeable increase in HepG2 cells by our detection method (C. Noguchi and K. Chayama, unpublished data). However, the method employed to detect hypermutation is not quantitative. Moreover, no antibody to detect APOBEC3G is available. Measurement of activity of this enzyme might be necessary to address this issue.

Because the patterns of hypermutations found in patients as well as cell lines are in agreement with strong dinucleotide preferences of a retroviral genome³¹⁻³⁵ edited by APOBEC3G,⁷⁻⁹ we assume that hypermutations might also be induced by a similar enzyme. As pointed out by Turelli et al.,²⁰⁻²⁹ another deaminase including APOBEC3F might be responsible for the generation of hypermutation. We actually detected the expression of deaminases in HepG2 cell lines. The expression levels of these deaminases are very low because they were detected by only two-stage PCR with one exception (only APOBEC3F was detected by a single-stage PCR).

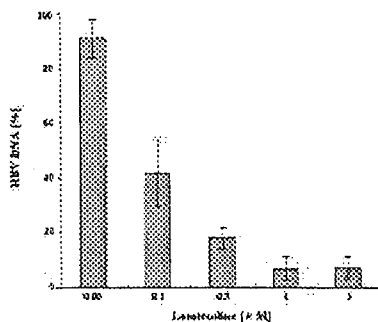


Fig. 7. Effects of lamivudine on production of HBV DNA by cell line 1. After 5 days of lamivudine treatment, the HBV DNA in core particles was immunoprecipitated and quantitated by real-time PCR. Data are mean \pm SD of 4 independent experiments.

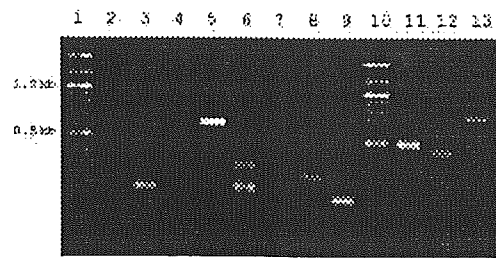


Fig. 8. Agarose gel electrophoresis of mRNAs of known deaminases amplified by reverse transcription-polymerase chain reaction. Lane 1: molecular weight size marker; lane 2: APOBEC1; lane 3: APOBEC2; lane 4: APOBEC3A; lane 5: APOBEC3B; lane 6: APOBEC3C; lane 7: APOBEC3D; lane 8: APOBEC3F; lane 9: APOBEC3G; lane 10: molecular weight size marker. Only mRNA of APOBEC3F was detected by one-stage PCR. To confirm the predictability of the assay, 3 negative mRNAs in Hep3G (APOBEC1, 3A and 3D) were amplified by using mRNAs from tissues known to express it. Lanes 11 and 12: APOBEC1 and APOBEC3A from the ileum; lane 13: APOBEC3D from the duodenum. All detected cDNAs were cloned, and nucleotide sequences were confirmed.

However, other possibilities should not be ignored. For example, some viral proteins might prevent such editing activity of deaminase by associating with this enzyme, as virion infectivity factor does in HIV-1-infected cells. Possibly the edited HBV genomes are degraded in liver cells rapidly by removal of the U residues by uracil DNA glycosylase followed by cellular nucleases.³⁶

We found hypermutated genomes only in patients positive for eAb. The G to A nucleotide substitution of codon 28 of pre-core protein, which induces premature stop of this protein and basal core promoter mutations (A1762T/G1764A), might be related to the clearance of eAg.²⁸ Further studies should be conducted to investigate the relationship between G to A substitutions in these regions by deaminase(s), production of eAg, and replication efficacy of the virus.

A recent study showed that the amount of HBV DNA reduction occurs noncytopathologically through the action of cytokines, especially interferon alpha/beta and gamma.^{37,38} We thus examined whether interferon can alter the occurrence of hypermutation. However, the results showed no increase in the number of hypermutation in HepG2-derived cell lines treated by interferon alpha and gamma (Fig. 6). Thus, the antiviral action of the mechanism responsible for G to A substitution in liver cells is likely to be independent of the action of interferon.

In conclusion, numerous innate intracellular defense systems exist, and the precise pathways of such systems are not fully understood. The role of editing of the HBV genome in such defense systems should be further investigated to understand the natural antiviral mechanisms and to develop an antiviral strategy against HBV.

Acknowledgment: A part of this work was carried out at the Research Center for Molecular Medicine, Faculty of Medicine, and Liver Research Project Center, Hiroshima University, Hiroshima, Japan. The authors thank thank Eiko Okutani, Yukiji Tonouchi and Kiyomi Toyota for their excellent technical assistance.

References

- Wright TL, Lau JY. Clinical aspects of hepatitis B virus infection. *Lancet* 1993;342:1340-1344.
- Bruix J, Llovet JM. Hepatitis B virus and hepatocellular carcinoma. *J Hepatol* 2003;39(Suppl 1):S59-S63.
- Raimondo G, Pollicino T, Squadrito G. Clinical virology of hepatitis B virus infection. *J Hepatol*. 2003;39(Suppl 1):S26-S30.
- Ganem D, Prince AM. Hepatitis B virus infection: Natural history and clinical consequences. *N Engl J Med* 2004;350:1118-1129.
- Ganem D, Schneider R. *Hepadnaviridae: The Virus and Their Replication*. Volume 3. 4th ed. Philadelphia: Lippincott-Raven Publishers, 2001.
- Skalka AM, Goff SP. *Reverse Transcriptase*. Cold Spring Harbor, NY: Cold Spring Harbor Laboratory Press, 1993.
- Mangeat B, Turelli P, Caron G, Friedli M, Perrin L, Trono D. Broad antiretroviral defense by human APOBEC3G through lethal editing of nascent reverse transcripts. *Nature* 2003;424:99-103.
- Zhang HYB, Pomerantz RJ, Zhang C, Arunachalam SC, Gao L. The cytidine deaminase CEM15 induces hypermutation in newly synthesized HIV-1 DNA. *Nature* 2003;424:94-98.
- Lecossier D, Bouchonnet F, Clavel F, Hance AJ. Hypermutation of HIV-1 DNA in the absence of the Vif protein. *Science* 2003;300:1112.
- Harris RS, Bishop KN, Sheehy AM, Craig HM, Petersen-Mahrt SK, Watt IN, et al. DNA deamination mediates innate immunity to retroviral infection. *Cell* 2003;113:803-809.
- Mariani R, Chen D, Schrofelbauer B, Navarro F, König R, Bollman B, et al. Species-specific exclusion of APOBEC3G from HIV-1 virions by Vif. *Cell* 2003;114:21-31.
- Kobayashi M, Takaori-Kondo A, Shindo K, Abudu A, Fukunaga K, Uchiyama T. APOBEC3G targets specific virus species. *J Virol* 2004;78:8238-8244.
- Shindo K, Takaori-Kondo A, Kobayashi M, Abudu A, Fukunaga K, Uchiyama T. The enzymatic activity of CEM15/Apobec-3G is essential for the regulation of the infectivity of HIV-1 virion but not a sole determinant of its antiviral activity. *J Biol Chem* 2003;278:44412-44416.
- Li J, Potash MJ, Volsky DJ. Functional domains of APOBEC3G required for antiviral activity. *J Cell Biochem* 2004;92:560-572.
- Liu B, Yu X, Luo K, Yu Y, Yu XF. Influence of primate lentiviral Vif and proteasome inhibitors on human immunodeficiency virus type 1 virion packaging of APOBEC3G. *J Virol* 2004;78:2072-2081.
- Mehle A, Strack B, Ancuta P, Zhang C, McPike M, Gabuzda D. Vif overcomes the innate antiviral activity of APOBEC3G by promoting its degradation in the ubiquitin-proteasome pathway. *J Biol Chem* 2004;279:7792-7798.
- Marin M, Rose KM, Kozak SL, Kabat D. HIV-1 Vif protein binds the editing enzyme APOBEC3G and induces its degradation. *Nat Med* 2003;9:1398-1403.
- Stopak K, de Noronha C, Yonemoto W, Greene WC. HIV-1 Vif blocks the antiviral activity of APOBEC3G by impairing both its translation and intracellular stability. *Mol Cell* 2003;12:591-601.
- Gunther S, Somner G, Plikat U, Irmaska A, Wain-Hobson S, Will H, et al. Naturally occurring hepatitis B virus genomes bearing the hallmarks of retroviral G→A hypermutation. *Virology* 1997;235:104-108.
- Turelli P, Mangeat B, Jost S, Vianin S, Trono D. Inhibition of hepatitis B virus replication by APOBEC3G. *Science* 2004;303:1829.
- Ohishi W, Shirakawa H, Kawakami Y, Kimura S, Kamiyasu M, Tazuma S, et al. Identification of rare polymerase variants of hepatitis B virus using a two-stage PCR with peptide nucleic acid clamping. *J Med Virol* 2004;72:558-565.
- Rose PP, Korber BT. Detecting hypermutations in viral sequences with an emphasis of G to A hypermutation. *Bioinformatics* 2000;16:400-401.
- Egholm M, Buchardt O, Christensen L, Behrens C, Freier SM, Driver DA, et al. PNA hybridizes to complementary oligonucleotides obeying the Watson-Crick hydrogen-bonding rules. *Nature* 1993;365:566-568.
- Cabrero M, Barolom J, Caramelo C, Barril G, Carreno V. Molecular analysis of hepatitis B virus DNA in serum and peripheral blood mononuclear cells from hepatitis B surface antigen-negative cases. *HEPATOLOGY* 2000;32:116-123.
- Cabrero M, Baetolome J, Carreno V. In vitro infection of human peripheral blood mononuclear cells by a defective hepatitis B virus with a deletion in the PreS1 region of the viral genome. *J Viral Hepatol* 2002;9:265-271.
- Zoulim F, Vitvitski L, Bouffard P, Pichoud C, Rougier P, Lamelin JP, et al. Detection of pre-S1 proteins in peripheral blood mononuclear cells from patients with HBV infection. *J Hepatol* 1991;12:150-156.
- Murakami Y, Minami M, Daimon Y, Okanoue T. Hepatitis B virus DNA in liver, serum, and peripheral blood mononuclear cells after the clearance of serum hepatitis B virus surface antigen. *J Med Virol* 2004;72:203-214.
- Milich D, Liang TJ. Exploring the biological basis of hepatitis B e antigen in hepatitis B virus infection. *HEPATOLOGY* 2003;38:1075-1086.
- Turelli P, Jost S, Mangeat B, Trono D. Response to comment of "Inhibition of hepatitis B virus replication by APOBEC3G". *Science* 2004;305:1403b.
- Rosler C, Kock J, Malim MH, Blum HE, Weizsacker F. Comment on "Inhibition of hepatitis B virus replication by APOBEC3G". *Science* 2004;305:1403a.
- Kouliniska I, Chaplin B, Mwagagile D, Essex M, Renjifo B. Hypermutation of HIV type 1 genomes isolated from infants soon after vertical infection. *AIDS Res Hum Retrov* 2003;19:1115-1123.
- Vartanian J, Meterhans A, Sala M, Wain-Hobson S. Selection, recombination, and G→A hypermutation of human immunodeficiency virus type 1 genomes. *J Virol* 1991;65:1779-1788.
- Janini M, Rogers M, Birx DR, McCutchan FE. Human immunodeficiency virus type 1 DNA sequences genetically damaged by hypermutation are often abundant in patient peripheral blood mononuclear cells and may be generated during near-simultaneous infection and activation of CD4+ T cells. *J Virol* 2001;75:7973-7986.
- Borman A, Quillent C, Charneau P, Kean KM, Clavel F. A highly defective HIV-1 group O provirus: evidence for the role of local sequence determinants in G→A hypermutation during negative-strand viral DNA synthesis. *Virology* 1995;208:601-609.
- Overbaugh J, Jackson S, Papenhausen M, Rudensey LM. Lentiviral genomes with G-to-A hypermutation may result from Taq polymerase errors during polymerase chain reaction. *AIDS Res Hum Retroviruses* 1996;17:1605-1613.
- Lindahl T, Wood RD. Quality control by DNA repair. *Science* 1999;286:1897-1905.
- Guidotti LG, Ando K, Hobbs MV, Ishikawa T, Runkel L, Schreiber RD, et al. Cytotoxic T lymphocytes inhibit hepatitis B virus gene expression by a noncytolytic mechanism in transgenic mice. *Proc Natl Acad Sci U S A* 1994;91:3764-3768.
- Guidotti LG, Ishikawa T, Hobbs MV, Matzke B, Schreiber R, Chisari FV. Intracellular inactivation of the hepatitis B virus by cytotoxic T lymphocytes. *Immunity* 1996;4:25-36.

Suppression of Macrophage Infiltration Inhibits Activation of Hepatic Stellate Cells and Liver Fibrogenesis in Rats

MICHIO IMAMURA,*† TADASHI OGAWA,* YASUYUKI SASAGURI,[§] KAZUAKI CHAYAMA,[†] and HIKARU UENO*

*Department of Biochemistry and Molecular Pathophysiology, University of Occupational and Environmental Health, School of Medicine, Kitakyushu, Japan; †Department of Medicine and Molecular Science, Graduate School of Biomedical Science, Hiroshima University, Hiroshima, Japan; and §Department of Pathology and Cell Biology, University of Occupational and Environmental Health, School of Medicine, Kitakyushu, Japan

Background & Aims: Monocytes/macrophages infiltrate into injured livers. We tried to clarify their roles in inflammation and subsequent fibrogenesis by inhibiting their infiltration with a mutated form (7ND; 7 amino acids at the N-terminal were deleted) of monocyte chemoattractant protein 1, which may function as a dominant-negative mutant. **Methods:** Rats were injected via the tail vein with an adenovirus expressing either human 7ND (Ad7ND), a truncated type II transforming growth factor β receptor (AdT β -TR), which works as a dominant-negative receptor, bacterial β -galactosidase (AdLacZ), or saline. Seven days later, the rats were treated with dimethylnitrosamine for 1–21 days. **Results:** Within 24 hours after a single dimethylnitrosamine injection, macrophages were observed in livers. With a 3-day dimethylnitrosamine treatment, activated hepatic stellate cells were detectable in livers in AdLacZ-, AdT β -TR-, and saline-injected rats. In contrast, in the Ad7ND-treated rats, infiltration of macrophages was markedly reduced, and activated hepatic stellate cells were not detectable. After a 3-week dimethylnitrosamine treatment, fibrogenesis was almost completely inhibited, and activated hepatic stellate cells were hardly seen in livers in both Ad7ND- and AdT β -TR-treated rats. **Conclusions:** Our results show that blockade of macrophage infiltration inhibits activation of hepatic stellate cells and leads to suppression of liver fibrogenesis. The presence of activated hepatic stellate cells in the initial phase after injury and its absence at a later phase in the AdT β -TR-treated livers indicate that transforming growth factor β is not an activating factor for hepatic stellate cells, and this suggests that transforming growth factor β is required for the survival of activated hepatic stellate cells. Our study suggests that infiltrated macrophages may themselves produce an activating factor for hepatic stellate cells.

Inflammation is always accompanied by an infiltration by leukocytes,¹ a process that is thought to be regulated by chemotactic cytokines called *chemokines*.^{1,2} Monocyte

chemoattractant protein (MCP)-1, one of these chemokines, induces infiltration by monocytes/macrophages and lymphocytes³ by binding to a specific receptor, CCR2.^{1,2} In animal models of liver injury^{4,5} and in patients with chronic hepatitis,^{6,7} MCP-1 is detectable in both livers and serum. Injury-induced inflammation results in tissue remodeling or liver fibrosis. However, the actual roles performed by infiltrated monocytes/macrophages and MCP-1 in liver fibrogenesis are largely unknown.

During liver fibrogenesis, hepatic stellate cells (HSC) are activated to myofibroblast-like cells expressing α -actin. These activated HSC and myofibroblasts already existing in the portal field and around central veins may play a central role in fibrogenesis,⁸ after which they produce extracellular matrix through the generation of various cytokines, including transforming growth factor (TGF)- β .⁹ For fibrogenesis, HSC are considered to be the responsible cells, and TGF- β is one of the critical factors for fibrogenesis. In fact, when we inhibited the action of TGF- β by using a dominant-negative mutated receptor for TGF- β ,¹⁰ the activated HSC were markedly reduced in number, and fibrogenesis, as well as the progression of already-established fibrosis, was almost completely suppressed.^{11–13} This shows the essential roles played by TGF- β and HSC in fibrotic remodeling after liver injury. However, the mechanism underlying the activation of HSC is not fully understood, although TGF- β has been believed to be an activating factor.¹⁴

In this study, to try to answer these questions, we introduced a mutated form of MCP-1 (7ND), which is

Abbreviations used in this paper: DMN, dimethylnitrosamine; ELISA, enzyme-linked immunosorbent assay; HSC, hepatic stellate cells; MCP, monocyte chemoattractant protein; MOI, multiplicity of infection; TGF, transforming growth factor; TUNEL, terminal deoxynucleotidyl transferase-mediated deoxyuridine triphosphate nick-end labeling.

© 2005 by the American Gastroenterological Association
0016-5085/05/\$30.00

doi:10.1053/j.gastro.2004.10.005

considered to inhibit the action of MCP-1 as a dominant-negative mutant,^{15,16} into dimethylnitrosamine (DMN)-treated rats, an established model of liver fibrosis with a pathology closely resembling that of human cirrhosis.^{17,18} Some rats were given a dominant-negative TGF- β receptor to eliminate signaling by TGF- β .^{11,12} We compared these rats in terms of (1) infiltration by monocytes/macrophages and activation of HSC, both of which occur in the acute phase after injury, and (2) fibrotic changes in the chronic phase after injury. Although inhibition of MCP-1 and blockade of TGF- β each led to a marked suppression of liver fibrogenesis, we were interested to find that some responses in the initial phase after injury were quite different between these 2 groups. Our study indicates that TGF- β is not an activating factor for HSC and suggests that infiltrated monocytes/macrophages may produce the activating factor(s).

Materials and Methods

Preparation of Adenoviruses

Replication-defective E1⁻ and E3⁻ adenoviral vectors expressing an amino-terminal deletion mutant of human MCP-1 (Ad7ND) with a FLAG epitope tag in its carboxyl-terminal (complementary DNA, a generous gift from Dr. B. Rollins, Harvard University),^{15,16} a truncated human TGF- β type II receptor (AdT β -TR),¹⁰⁻¹² or bacterial β -galactosidase (AdLacZ)¹⁹ under a CA promoter comprising a cytomegalovirus enhancer and a chicken β -actin promoter²⁰ were prepared as previously described.²¹

Detection of Mutated Human Monocyte Chemoattractant Protein 1 (7ND) and Rat Wild-Type Monocyte Chemoattractant Protein 1

COS cells were infected with either Ad7ND (multiplicity of infection [MOI] of 1, 10, and 100) or AdLacZ (MOI of 10), as previously described.¹⁰ One day after infection, the medium was replaced with serum-free medium, and cells were incubated for a further 24 hours. A mutant MCP-1 (7ND) secreted into culture media was analyzed by Western blotting by using monoclonal antibodies against either FLAG (Abcam, Cambridge, UK) or human MCP-1 (Sanbio, 5400 AM Uden, The Netherlands), as previously described.¹³

7ND and rat MCP-1 were also detectable by enzyme-linked immunosorbent assay (ELISA). Livers were homogenized in phosphate-buffered saline with 1% Triton X-100, 0.1% sodium dodecyl sulfate, and 0.5% sodium deoxycholate. The homogenates were centrifuged at 20,000g for 30 minutes. 7ND and rat MCP-1 were measured in the supernatant of liver homogenates and in sera from rats by using a human MCP-1 ELISA kit (Biosource, Camarillo, CA) and a rat kit (Biosource), respectively, according to the manufacturer's instructions. These ELISA kits are species specific, and cross-reaction be-

tween human and rat MCP-1 is less than 5%. In fact, no human MCP-1 protein was detectable in samples from either intact or AdLacZ-infected rats (data not shown).

Animal Models

All animals were treated under protocols approved by the institutional animal care committees, and the experiment was performed under both the institutional guidelines for animal experiments and by the Law (No. 105) and Notification (No. 6) of the Japanese government. Male Sprague-Dawley rats, 10 weeks old and weighing approximately 350 g, were given a single infusion of 0.5 mL of Ad7ND, AdT β -TR, AdLacZ (2×10^9 plaque-forming units per milliliter), or saline via the tail vein, as previously reported.¹² By this method, virtually all cells in the liver were infected and expressed the introduced molecule.^{11,12} Seven days later, rats were given an intraperitoneal injection of DMN (10 μ g/g body weight; Wako, Osaka, Japan) either once or at the indicated times (3 consecutive daily injections or 3 consecutive daily injections and 4 days off per week for 3 weeks), as previously reported.¹¹⁻¹³ After DMN treatment, blood was collected, and the rats were killed. Biochemical parameters were measured by using standard methods. The liver was either fixed with 4% buffered paraformaldehyde for histological examination or frozen immediately in liquid nitrogen for the extraction of hydroxyproline, the content of which was measured as described elsewhere.²²

Histological Examination

Liver sections were stained with hematoxylin or Masson trichrome or subjected to immunohistostaining by using antibodies against either CD68 (ED-1; Serotec, Raleigh, NC) or α -actin (Dako, Tokyo, Japan). Immunoreactive materials were visualized by using a streptavidin-biotin staining kit (Histofine SAB-PO kit; Nichirei, Tokyo, Japan) and diaminobenzidine. Macrophages (CD68-positive cells) and lymphocytes were counted by a technician blinded to the treatment regimen. Four random high-power (200 \times) fields from each section were examined. As negative controls, immunohistostaining was performed without the first antibodies.

Determination of Hepatic Stellate Cells in Apoptosis

Fragmented DNA in apoptotic cells in liver sections was stained with diaminobenzidine (dark brown) by the terminal deoxynucleotidyl transferase-mediated deoxyuridine triphosphate nick-end labeling (TUNEL) technique by using a commercially available kit (Roche Diagnostics, Mannheim, Germany). Then, the sections were double-stained against α -actin and visualized with the aid of 3-amino-9-ethyl carbazole liquid substrate chromogen (red; Dako). As negative controls, the TUNEL reaction mixture was used without terminal transferase.

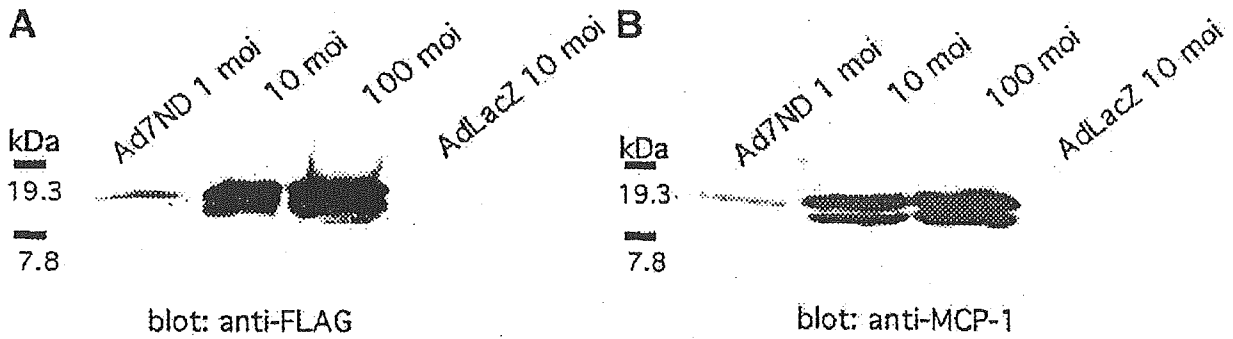


Figure 1. A mutated form of MCP-1 (7ND) is secreted from cells infected with Ad7ND. COS cells were infected either with Ad7ND or with AdLacZ at the indicated MOI. After 48 hours, the culture media were subjected to sodium dodecyl sulfate-polyacrylamide gel electrophoresis (12%) and analyzed by Western blotting by using antibodies against either (A) FLAG or (B) human MCP-1. Molecular markers are in kilodaltons.

Statistical Analysis

Statistical analysis was performed by 1-way analysis of variance followed by Scheffé's test. *P* < .05 was considered significant.

Results

A Mutant Monocyte Chemoattractant Protein 1, 7ND, Was Secreted From Ad7ND-Infected Cells and Detected in the Serum and Liver of Ad7ND-Infected Rats

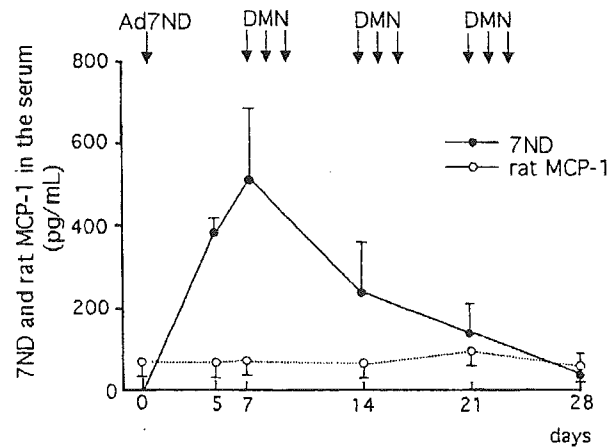
In the culture medium from Ad7ND-infected COS cells, 7ND was readily detectable in an MOI-dependent manner, as assessed by Western blotting analysis (Figure 1). Human 7ND and endogenous rat MCP-1 proteins were measured in sera (Figure 2A) and liver

extracts (Figure 2B) from rats infected with Ad7ND. Seven days after gene transfer, a 3-week DMN treatment was begun. It is interesting to note that the amount of rat MCP-1 was not significantly changed by DMN treatment in either serum or liver. 7ND reached a peak on the seventh day after gene transfer and then declined gradually; however, the values were much higher than those obtained for rat MCP-1 in most time periods under DMN injury.

Dimethylnitrosamine-Induced Infiltration by Macrophages and Lymphocytes and Activation of Hepatic Stellate Cells Were Both Suppressed in Ad7ND-Treated Livers

Rats were infused via the tail vein with either saline or an adenovirus expressing 1 of the following:

A (serum)



B (liver)

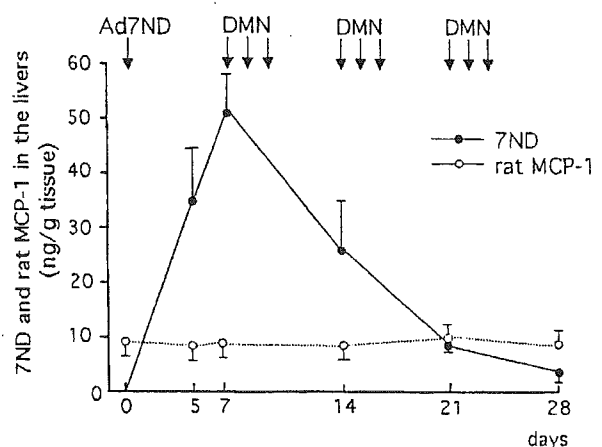


Figure 2. Amounts of human 7ND and rat MCP-1 in the sera (A) and livers (B) of DMN-injured rats. Rats were given a single infusion of Ad7ND (or saline infusion) via the tail vein. Seven days later, rats were subjected to a 3-week DMN treatment (shown as arrows). Rats were killed 5, 7 (just before the initiation of DMN treatment), 14, 21, and 28 days after Ad7ND injection. Means \pm SD (*n* = 4) are shown.